

Università degli Studi di Napoli “Federico II”



**SCUOLA POLITECNICA E DELLE SCIENZE DI BASE
DIPARTIMENTO DI INGEGNERIA INDUSTRIALE**

**CORSO DI LAUREA IN INGEGNERIA AEROSPAZIALE
CLASSE DELLE LAUREE IN INGEGNERIA INDUSTRIALE (L-9)**

Elaborato di laurea in Meccanica del Volo
**Geometric modelling and static stability analysis of
the Canadair water bomber with JPAD and
OpenVSP.**

**Relatore:
Prof. Danilo Ciliberti**

**Candidato:
Salvatore Trepiccione
Matr. N35003217**

ANNO ACCADEMICO 2021 – 2022

*Alla mia famiglia.
E a tutti coloro che, durante questo percorso, hanno contribuito alla mia formazione.*

Abstract

The purpose of the following work is to perform modeling of the Viking Air 415 Superscooper aircraft better known as "Canadair CL-415" using JPAD software, which is followed by stability and control analysis using the OpenVSP suite. JPAD (Java toolchain of Programs for Aircraft Design) is a comprehensive integrated software for aircraft design and offers a user-experience designed to follow the designer from the aircraft specification through the multidisciplinary analysis and optimization process. OpenVSP is an open-source parametric tool for aircraft geometry, originally developed by NASA. It can be used to create 3D models of aircraft and to support engineering analysis of those models. A key tool for analysis is VSPAERO, a fast, linear, lattice-based vortex solver that is used, in this paper, for the stability analysis. Discrete vortices are applied to each panel generated in the OpenVSP degenerate geometry file and then evaluated over the entire surface to obtain a pressure and thus force distribution.

Sommario

Lo scopo del seguente lavoro è l'esecuzione della modellizzazione del velivolo Viking Air 415 Superscooper meglio noto come "Canadair CL-415" attraverso il software JPAD, a cui segue l'analisi di stabilità e controllo con la suite OpenVSP. JPAD (Java toolchain of Programs for Aircraft Design) è un software integrato e completo per la progettazione di aeromobili ed offre una user-experience ideata per seguire il progettista dalle specifiche dell'aeromobile fino al processo di analisi e ottimizzazione multidisciplinare. OpenVSP è uno strumento parametrico open source per la geometria dei velivoli, originariamente sviluppato dalla NASA. Può essere utilizzato per creare modelli 3D di aerei e per supportare l'analisi ingegneristica di tali modelli. Strumento fondamentale per le analisi è VSPAERO, un solutore veloce, lineare e a reticolo di vortici che viene utilizzato in questo lavoro per l'analisi di stabilità. I vortici discreti vengono applicati a ciascun pannello generato nel file di geometria degenerata OpenVSP e quindi valutati sull'intera superficie per ottenere una distribuzione della pressione e quindi della forza.

Table of contents

List of figures	5
List of tables	7
1. Introduction	8
1.1 Objectives	8
1.2 Design of Seaplanes	8
1.3 Layout of the work	10
2. Theoretical aspects	11
3. JPAD	15
4. Aerodynamic analysis software	20
4.1 OpenVSP	20
4.2 VSPAERO	21
5. Geometry and study of the wing	23
5.1 Geometry	23
5.2 Chordwise and Spanwise Refinement	25
6. Geometry and study of the vehicle	29
6.1 Geometry modelling in OpenVSP	29
6.2 Results and discussion	36
7. Conclusions	49
Bibliography	50

List of figures

Figure 1.1 A floatplane configuration.	9
Figure 1.2 An amphibious configuration.....	9
Figure 1.3 A Viking Air 415 with the insignia of the Italian Civil Defense Department in action.	10
Figure 2.1 Analysis of the profile by decomposition	12
Figure 2.2 The figure shows the velocity (dV) induced at a point P by an element of vortex filament (dl) of strength Γ	13
Figure 2.3 Schematic of one single horseshoe vortex.	14
Figure 2.4 Types of wing planforms for which the classical lifting-line theory is not sufficient.	15
Figure 3.1 Data Tables took from "Janes All the World's Aircraft: Development & Production Yearbook 04/05" [2].	15
Figure 3.2 Canadair CL-415 aircraft triptych.....	16
Figure 3.3 JPAD Modeller graphical user interface.	16
Figure 3.4 Equivalent lifting surface-wing and Top view-fuselage.	17
Figure 3.5 Equivalent lifting surface-horizontal tail and Equivalent lifting surface-vertical tail.	18
Figure 3.6 Side view-nacelle and Side view-starboard tip float.....	18
Figure 3.7 views comparisons.	20
Figure 4.1 OpenVSP setup: To the left we have the Workspace, to the middle the Geometry browser, to the right the Geometry window	21
Figure 4.2 VSPAERO-Overview tab.....	22
Figure 5.1 In the first image we have the wing (without sub-surfaces) visualized in OpenVSP, in the second the wing and profile parameters (plan and airfoil), in the last the NACA profile took from http://airfoiltools.com	24
Figure 5.2 CL vs Num_W, $\alpha = 6^\circ$	25
Figure 5.3 CD vs Num_W, $\alpha = 6^\circ$	26
Figure 5.4 CM_y vs Num_W, $\alpha = 6^\circ$	26
Figure 5.5 CL vs Num_U, $\alpha = 6^\circ$	27
Figure 5.6 CD vs Num_U, $\alpha = 6^\circ$	28
Figure 5.7 CM_y vs Num_U, $\alpha = 6^\circ$	28

Figure 6.1 Aircraft visualized in OpenVSP (view comparison).....	29
Figure 6.2 Aircraft visualized in OpenVSP (Surface “Hidden”).....	30
Figure 6.3 Gen and XSec panels for fuselage sections.	31
Figure 6.4 Plan panel for horizontal tail.	32
Figure 6.5 Airfoil panel for horizontal tail.	32
Figure 6.6 NACA 0012 profile took from http://airfoiltools.com	33
Figure 6.7 Plan panel for vertical tail.	33
Figure 6.8 XForm and Design panel for nacelle and propeller.	34
Figure 6.9 XForm panel for pod.....	34
Figure 6.10 Sub panel for: wing, horizontal tail and vertical tail.....	35
Figure 6.11 VSPAERO Overview panel.	36
Figure 6.12 CL vs AoA plot as flap deflection changes.....	38
Figure 6.13 CL vs CD plot as flap deflection changes.....	38
Figure 6.14 CM_y vs AoA plot as flap deflection changes, Vehicle CG (7.88,0,2.02).....	39
Figure 6.15 L/D vs AoA plot as flap deflection changes.	39
Figure 6.16 Solution Case 1, flap=0°, Alpha = 0°	40
Figure 6.17 Solution Case 4, flap=0°, Alpha = 10°	40
Figure 6.18 Solution Case 1, flap=15°, Alpha = 0°.....	41
Figure 6.19 Solution Case 4, flap=15°, Alpha = 10°.....	41
Figure 6.20 Solution Case 1, flap=30°, Alpha = 0°.....	42
Figure 6.21 Solution Case 4, flap=30°, Alpha = 10°.....	42
Figure 6.22 Load Distributions ranging with flap deflections. The lower curves refer to the tailplane. Note the downwash effect on the horizontal tail load due to the flap.	45
Figure 6.23 VSPAERO Advanced panel.....	46
Figure 6.24 VSPAERO Control Grouping panel.	47

List of tables

Table 6.1 Table of coefficients, flap=0°	37
Table 6.2 Table of coefficients, flap=15°	37
Table 6.3 Table of coefficients, flap=30°	37
Table 6.4 Overview Table, AoA=6.7°	44
Table 6.5 Table of angle increments.	48
Table 6.6 Table of all derivatives.	49

1. Introduction

1.1 Objectives

The objective of this thesis work is the modeling of the Canadair CL-415 aircraft and the subsequent use of VSPAERO as a vortex lattice solver. The first step is addressed with the help of JPAD, in fact by entering the different parameters related to the real geometry of the aircraft it was possible to create the CAD model from which the study started, exporting it appropriately, on the OpenVSP platform. From here it was considered the single wing through graphs obtained with Microsoft Excel and related to the trend of Lift coefficient, Moment coefficient, aerodynamic efficiency obtained as the angle of attack varies and the drag polar curves. At the end, the analysis is conducted similarly for the whole aircraft by inserting another point of view related to the variation of the deflection angle of the flaps. The study will be concluded with the application of codes formulated in MATLAB suitable to calculate the performance of the flap. The study will conclude with the application of codes formulated in MATLAB to calculate some performance of the aircraft under consideration.

1.2 Design of Seaplanes

The term seaplane is used for an airplane designed to operate from water. Generally, there are three kinds of seaplanes: floatplanes, flying boats, and amphibians. A floatplane is effectively a landplane that has had its landing gear removed and replaced with pontoons that are partially submerged floats (see Figure 1.1). Such floats place the fuselage well above the water surface. A flying boat is a type of seaplane in which the occupants and freight is carried inside a fuselage specifically designed to function as a hull for operation on the water. For this reason, they are also called hull seaplanes.

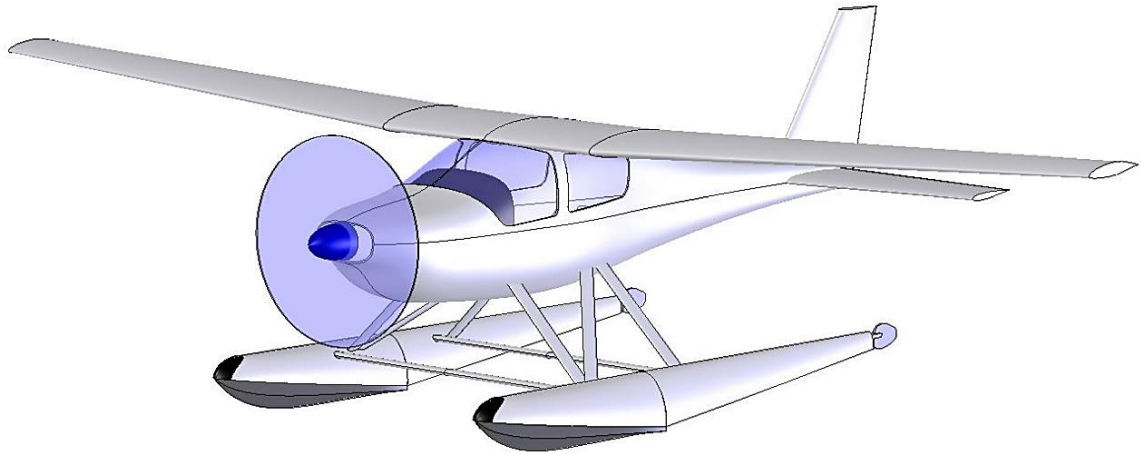


Figure 1.1 A floatplane configuration.

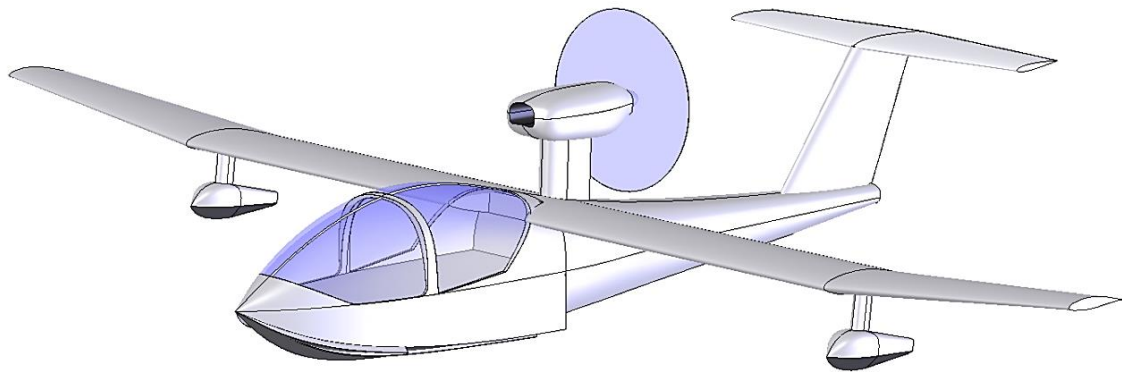


Figure 1.2 An amphibious configuration.

An amphibian is an aircraft that features a hull-type fuselage for water operations and retractable landing gear to allow landings to be made on land (see Figure 1.2).

The Canadair CL-415 (Super Scooper, later Bombardier 415) and the De Havilland Canada DHC-515 are a series of amphibious aircraft built originally by Canadair and subsequently by Bombardier and Viking Air, and De Havilland Canada. The CL-415 is based on the Canadair CL-215 and is designed specifically for aerial firefighting; it can perform various other roles, such as search and rescue and utility transport (see Figure 1.3).



Figure 1.3 A Viking Air 415 with the insignia of the Italian Civil Defense Department in action.

1.3 Layout of the work

Chapter 2: this chapter is shown to summarize all the fundamental theoretical aspects concerning aerodynamic analyses performed with VSPAERO. In VSPAERO, the user has a choice between two methods, the first is the Vortex Lattice Method (VLM) and the second one is a Panel Method; the focus will be on the first of the two methods listed.

Chapter 3: this chapter introduces JPAD in all its facets and functionalities, especially those that enabled the creation of the aircraft.

Chapter 4: this chapter discusses OpenVSP and the VSPAERO setup.

Chapter 5: this chapter represents the beginning of the study of the aircraft components, particularly the wing. Refinement is conducted in both chordwise and spanwise modes through iterations.

Chapter 6: this is the last chapter of analysis and focuses on the results obtained by using the various programs already mentioned, collecting the various outputs on excel sheets reorganized into appropriate graphs.

Chapter 7: Conclusions chapter.

2. Theoretical aspects

Starting with irrotational flow, which is defined as a flow where the vorticity ξ is zero at every point

$$\xi = \nabla \times V = 0 \tag{2.1}$$

If ϕ is a scalar function, following the vector identity, it follows that

$$\nabla \times (\nabla\phi) = 0 \tag{2.2}$$

Which means that the curl of the gradient of a scalar function is equal to zero. Combining the last two equations, gives

$$V = \nabla\phi \tag{2.3}$$

In this discussion ϕ is denoted as the velocity potential. From the principle of mass conservation for an incompressible flow, the equation (2.4) indicates that even though a fluid flows freely, its **density stays constant**.

$$\nabla \cdot V = 0 \tag{2.4}$$

By combining the equation (2.3) and (2.4), so considering an incompressible and irrotational flow it can be achieved the well-known Prandtl-Glauert Equation.

$$\nabla \cdot (\nabla\phi) = 0$$

(2.5)

$$\text{or } \nabla^2 \phi = 0$$

Since the Laplace's Equation is linear, it states that: a complicated flow pattern for an irrotational, incompressible flow can be summed up by adding together several elementary flows which in the same previous hypothesis. These different elementary flows include point/line source, point/line sink, point/line doublet and point/line vortex. The VLM is based on these line vortices.

Considering a symmetrical airfoil, the camber effect can also be neglected, after applying this boundary condition to Laplace's Equation, the problem can easily be solved by including the effect of angle of attack on a flat surface. Considering a wing placed on the x-y plane with a moderate angle of attack, the boundary condition states that normal flow across the thin wing's solid surface is zero

$$\nabla(\phi + \phi_\infty) = 0$$

(2.6)

From that equation it follows that the sum of the normal velocity component induced by the wing's bound vortices w_b , by the wake w_i and by the free-stream velocity V_∞ will be zero.

$$w_b + w_i + V_\infty \cdot \alpha = 0$$

(2.7)

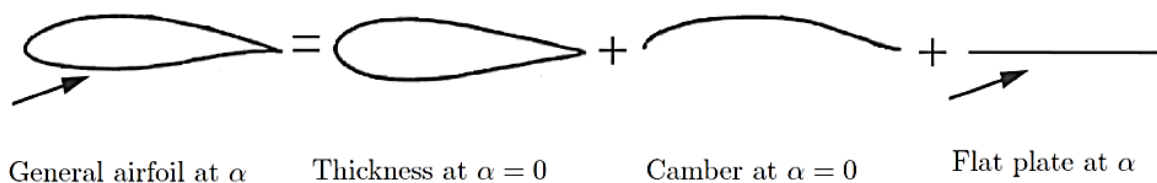


Figure 2.1 Analysis of the profile by decomposition

In two dimensions, for a vortex line of infinite length, the induced velocity at a point is given by

$$V_{\theta} = \frac{\Gamma}{2 \cdot \pi \cdot r} \quad (2.8)$$

Where Γ is the vortex circulation strength, r is the perpendicular distance between the point and the vortex line. The circulation has the same sign as its vorticity, so it is positive in the clockwise direction. The idea of a point vortex can be extended to a general three-dimensional vortex filament. The mathematical description of the flow induced by this filament is given by the Biot-Savart law. It states that the increment of the velocity dV at a point P due to a segment of a vortex filament dl at a point Q is.

$$dV_P = \frac{\Gamma}{4\pi} \cdot \frac{dl \times r_{PQ}}{|r_{PQ}|^3} \quad (2.9)$$

This can then be integrated over the entire length of the vortex filament to obtain the induced velocity in point P

$$V_P = \frac{\Gamma}{4\pi} \int \frac{dl \times r_{PQ}}{|r_{PQ}|^3} \quad (2.10)$$

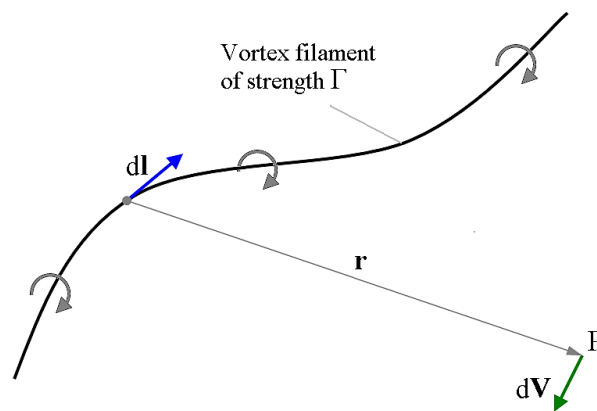


Figure 2.2 The figure shows the velocity (dV) induced at a point P by an element of vortex filament (dl) of strength Γ .

According to the Kutta-Joukowski Theorem, which states that a vortex of certain circulation Γ moving with free-stream velocity V_∞ creates lift L

$$L = \rho \cdot V_\infty \cdot \Gamma$$

In VLM the simplified case of the vortex ring used is the horseshoe vortex, shown in Figure 2.3, where the vortex line is assumed to be placed in the x-y plane.

$$V = V_{bc} + V_{b\infty} + V_{c\infty}$$

It consists of four vortex filaments. Two trailing segments ab and cd of the vortex are placed parallel to the direction of the free-stream velocity and start at infinity. The other two segments bc and ad are finite. The VLM models the lifting surfaces as an infinitely thin sheet of discrete vortices to compute lift L , induced drag D_i , lift curve slope, and lift distribution. The velocities induced by each horseshoe vortex at a specified control point are calculated using the law of Biot-Savart. A summation is performed for all control points on the wing, to produce a set of linear algebraic equations for the strength of each horseshoe vortex that satisfies the boundary condition of no flow through the wing (or model). The vortex strengths Γ_n are related to the wing circulation and the pressure differential between the upper and lower wing surfaces.

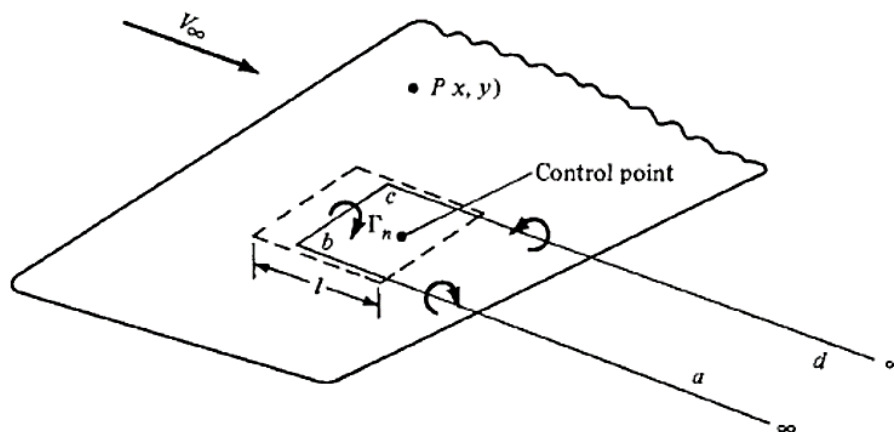


Figure 2.3 Schematic of one single horseshoe vortex.

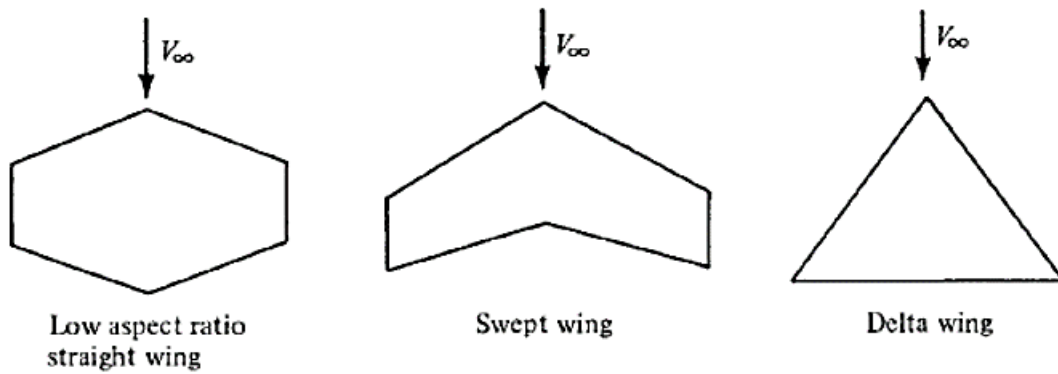


Figure 2.4 Types of wing planforms for which the classical lifting-line theory is not sufficient.

While VLM is based on horseshoe vortices, VSPAERO is characterized by a ring of vortices and only the tail vortices extend to infinity.

3. JPAD

The first step taken was to consider consistent data from which to perform the modeling of the aircraft in JPAD: specific features such as external dimensions and areas were taken from

DIMENSIONS, EXTERNAL:	
Wing span	28.63 m (93 ft 11 in)
Wing chord, constant	3.54 m (11 ft 7½ in)
Wing aspect ratio	8.2
Length overall	19.82 m (65 ft 0½ in)
Beam (max)	2.59 m (8 ft 6 in)
Length/beam ratio	7.5
Height overall: on land	9.07 m (29 ft 9 in)
on water	6.96 m (22 ft 10 in)
Draught: wheels up	1.12 m (3 ft 8 in)
wheels down	2.03 m (6 ft 8 in)
Tailplane span	10.97 m (36 ft 0 in)
Wheel track	5.25 m (17 ft 2¾ in)
Wheelbase	7.23 m (23 ft 8½ in)
Propeller diameter	3.97 m (13 ft 0¼ in)
Propeller fuselage clearance	0.59 m (1 ft 11¼ in)
Propeller water clearance	1.16 m (3 ft 9¼ in)
Propeller ground clearance	2.77 m (9 ft 1 in)
Forward door: Height	1.37 m (4 ft 6 in)*
Width	1.03 m (3 ft 4 in)
Height to sill	1.68 m (5 ft 6 in)
Rear door: Height	1.12 m (3 ft 8 in)
Width	1.02 m (3 ft 4 in)
Height to sill	1.83 m (6 ft 0 in)
Optional large rear cargo door:	
Height	1.12 m (3 ft 8 in)
Width	1.47 m (4 ft 10 in)
Height to sill	1.83 m (6 ft 0 in)
Water drop door: Length	1.60 m (5 ft 3 in)
Width	0.28 m (0 ft 11 in)
Emergency exit: Height	0.91 m (3 ft 0 in)
Width	0.51 m (1 ft 8 in)

"Janes All the World's Aircraft: Development & Production Yearbook 04/05" [2] while the creation and verification of geometry was done by assuming reference views of the aircraft.

AREAS:	
Wings, gross	100.33 m ² (1,080.0 sq ft)
Ailerons (total)	8.05 m ² (86.60 sq ft)
Flaps (total)	22.39 m ² (241.00 sq ft)
Fin	11.22 m ² (120.75 sq ft)
Rudder, incl tabs	6.02 m ² (64.75 sq ft)
Tailplane	20.55 m ² (221.20 sq ft)
Elevators (total, incl tabs)	7.88 m ² (84.80 sq ft)

Figure 3.1 Data Tables took from "Janes All the World's Aircraft: Development & Production Yearbook 04/05" [2].

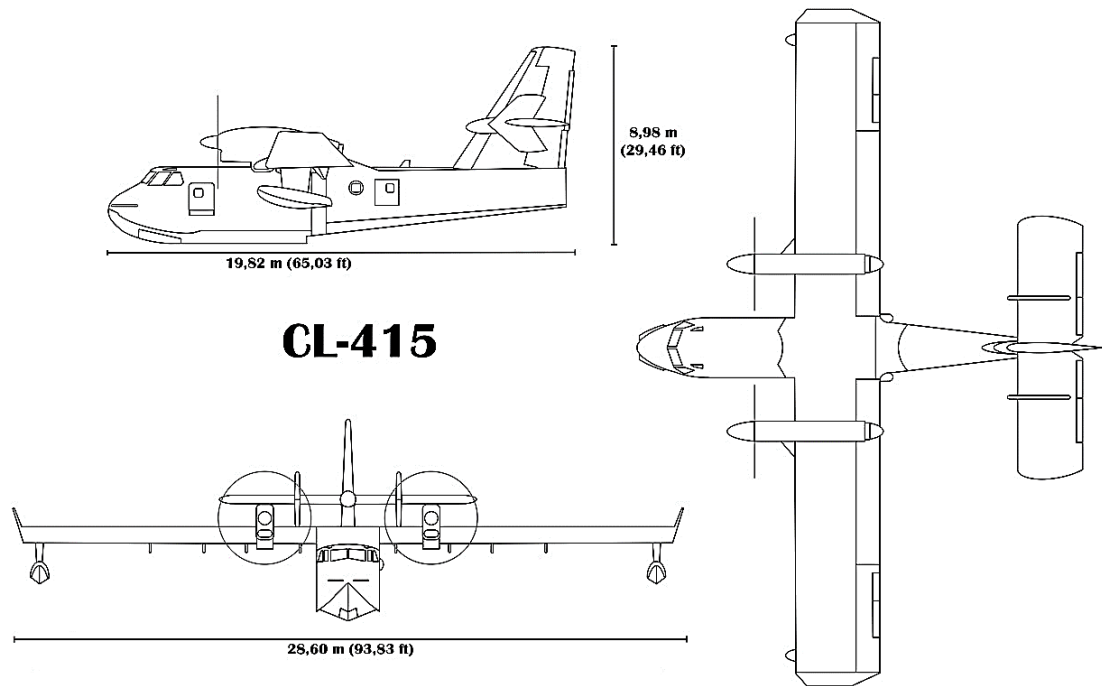


Figure 3.2 Canadair CL-415 aircraft triptych.

Therefore, the above data are essential to have a consistent geometry with that of the real aircraft. Once grouped all the specifications, necessary to give a correct representation of the aircraft, you can switch to the JPAD interface which is divided into two sides : on the left side you proceed to the generation of individual components by giving appropriate inputs related to dimensions and positioning, while on the right side you can view in real time the geometries created by the values chosen on the 3D explorer and specifically through a useful CAD model.

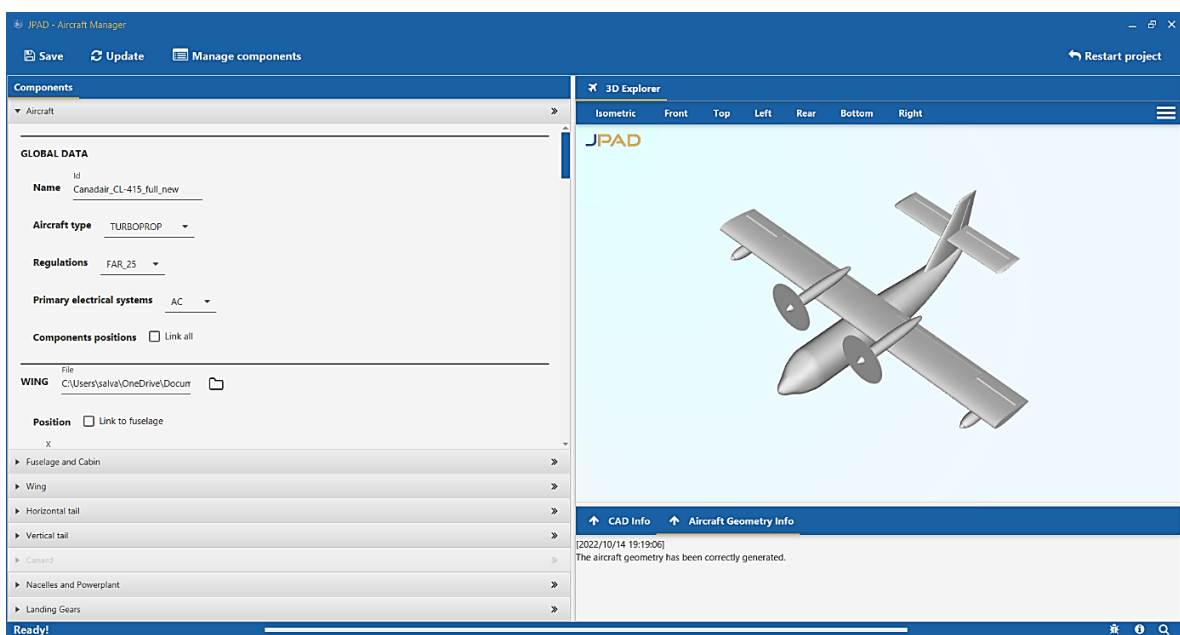


Figure 3.3 JPAD Modeller graphical user interface.

To add/delete components one must use the "Manage components" section in the upper left corner and then press on the "update" button near to it to have the required changes made; sometimes a problem was encountered during the change it will be JPAD itself that will alert the user with a warning message that appears post process. With JPAD it is possible to take action on components like:

- wing to add flaps, slats, ailerons or even winglets;
- fuselage to change the shape starting from a circle geometry;
- nacelles to obtain, in this case, the turboprop configuration;
- propeller diameter and thickness parameters;
- horizontal and vertical tail planes with associated control surfaces.

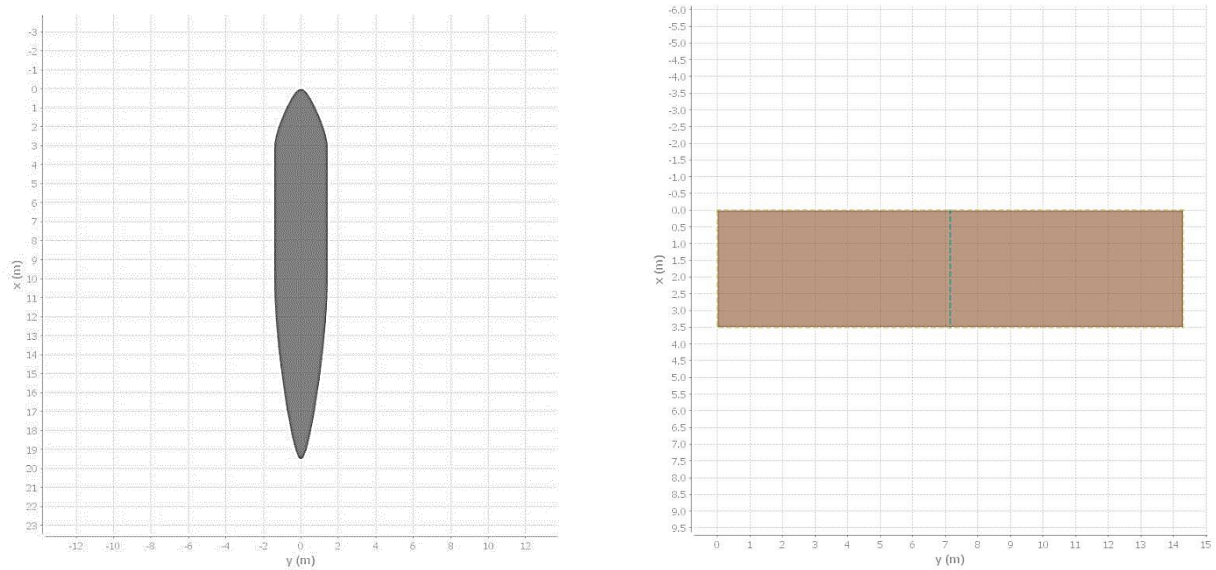


Figure 3.4 *Equivalent lifting surface-wing and Top view-fuselage.*

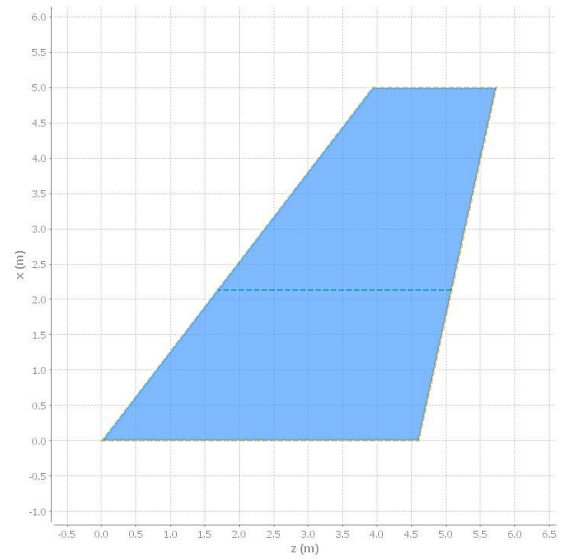
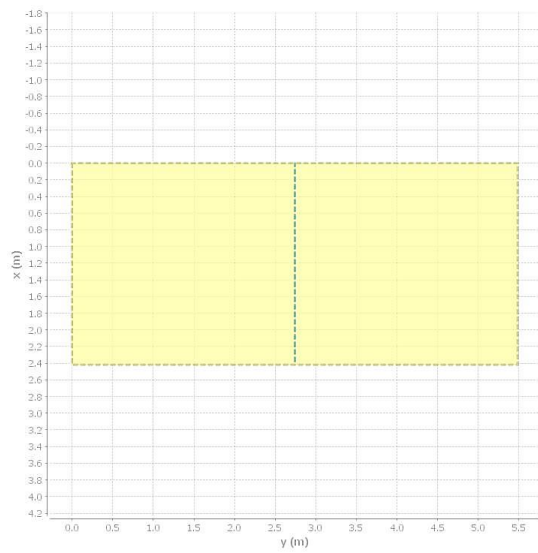


Figure 3.5 *Equivalent lifting surface-horizontal tail and Equivalent lifting surface-vertical tail.*

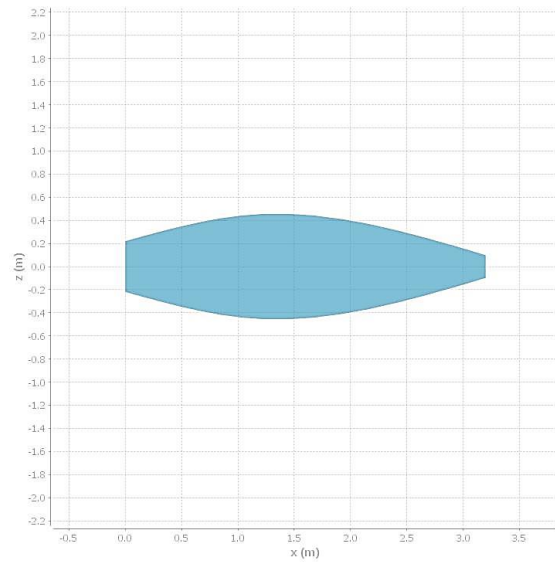
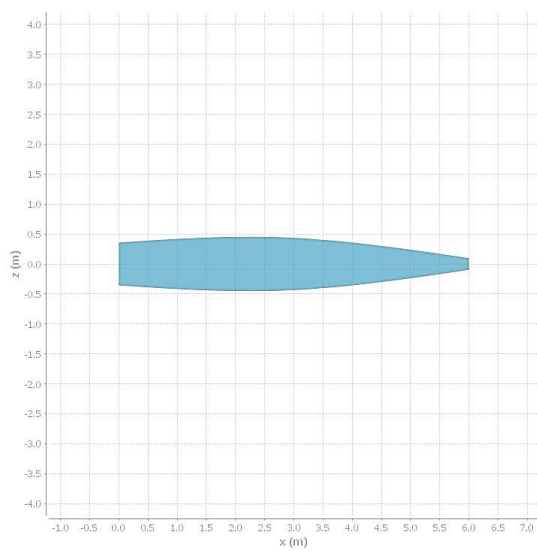
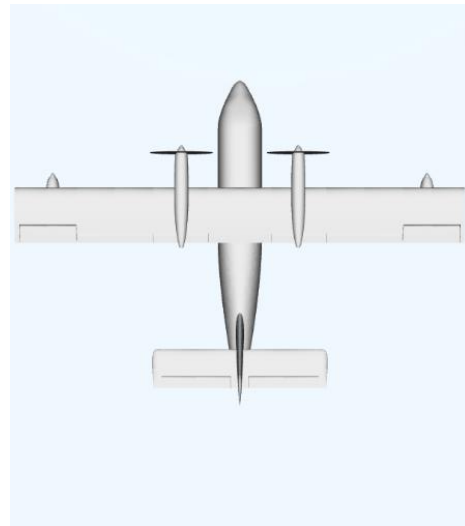
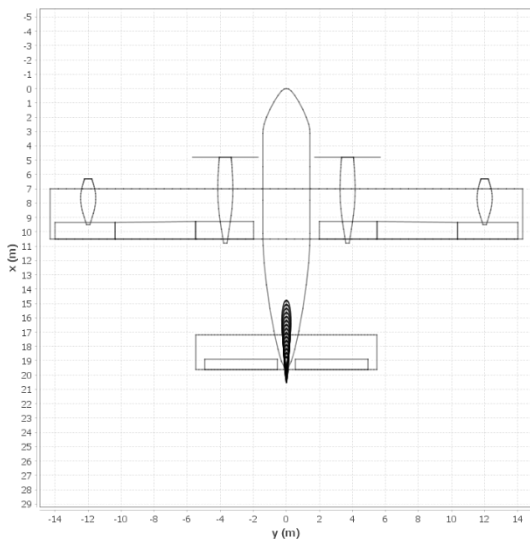
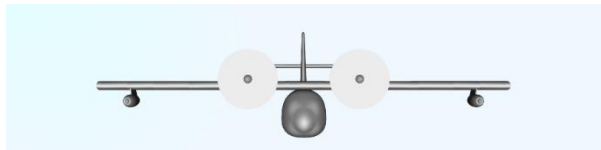
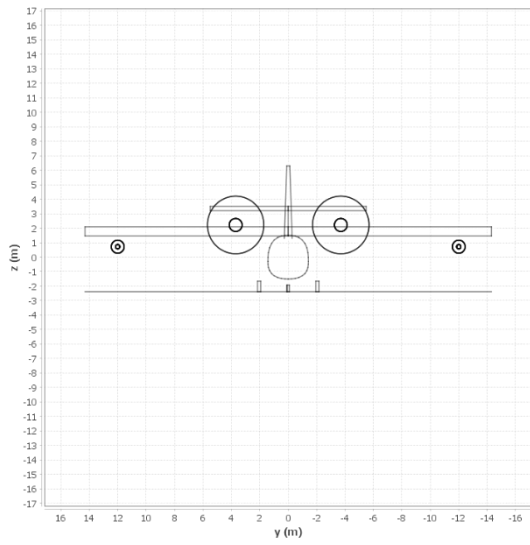


Figure 3.6 *Side view-nacelle and Side view-starboard tip float.*



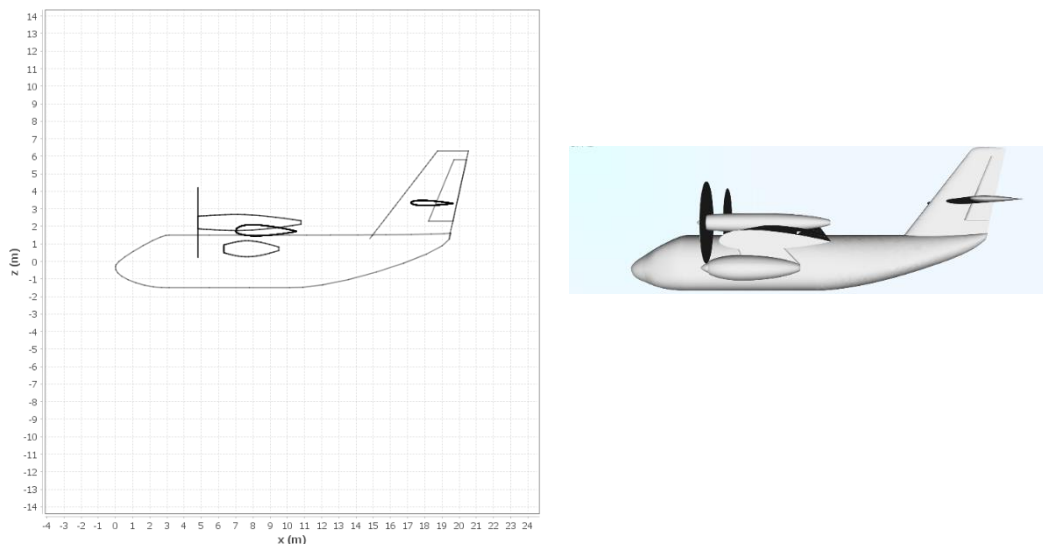


Figure 3.7 views comparisons.

Once the model is complete, the file is saved as an .xml and then the conversion can be made to a .vsp3, which allows us to transfer the product obtained in JPAD to the OpenVSP suite and then perform the longitudinal stability analysis.

4. Aerodynamic analysis software

4.1 OpenVSP

OpenVSP is the open-source parametric program that was used within this paper, in fact it allows the user to create a 3D model of an aircraft defined by common engineering parameters. This model can be processed in formats suitable for engineering analysis. On January 10, 2012, OpenVSP was released as an open-source project under the NASA Open-Source Agreement (NOSA) version 1.3. The program presents itself upon opening through a large initial panel on which appears, if the VSP3 format file of the aircraft has been loaded, the representation of the

aircraft next to which is the Geometry Browser with which one can access the parameters that allow one to modify the geometry of the aircraft.

The Geometry Browser lists all individual components (pod, fuselage, wing, stack, blank, ellipsoid, body of revolution, human, prop, hinge, conformal) of the user's model, while the workspace is where the model is displayed. When a component is selected, a component geometry window opens. This window is used to modify the parameters of the selected component.

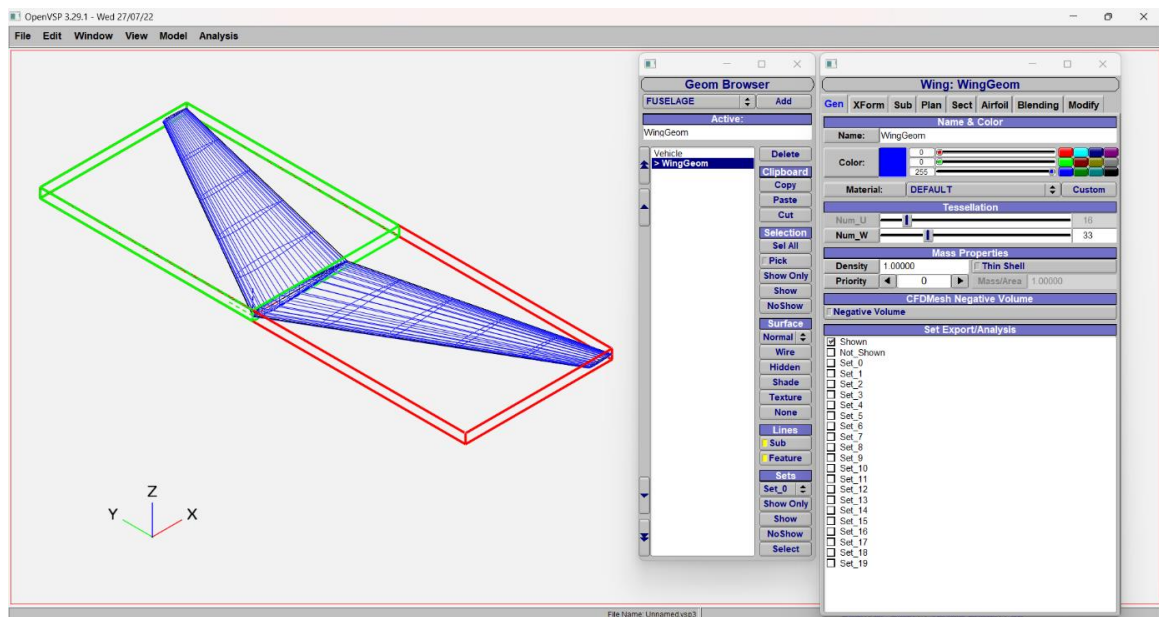


Figure 4.1 OpenVSP setup: To the left we have the Workspace, to the middle the Geometry browser, to the right the Geometry window

4.2 VSPAERO

VSPAERO is a linear solver that analyzes almost any geometry as long as the components are closed. It is a tool that will help to find most of the aerodynamic characteristics of a model based on a given set of conditions that fall within "normal" flight conditions (e.g., cruise, small angles of attack and sideslip), which it can then modify based on the physical limits or flight conditions being referenced. The degenerate geometry file is required if running VSPAERO's vortex lattice solver. Degenerate geometry files are representations of three-dimensional models in progressively simple frames.

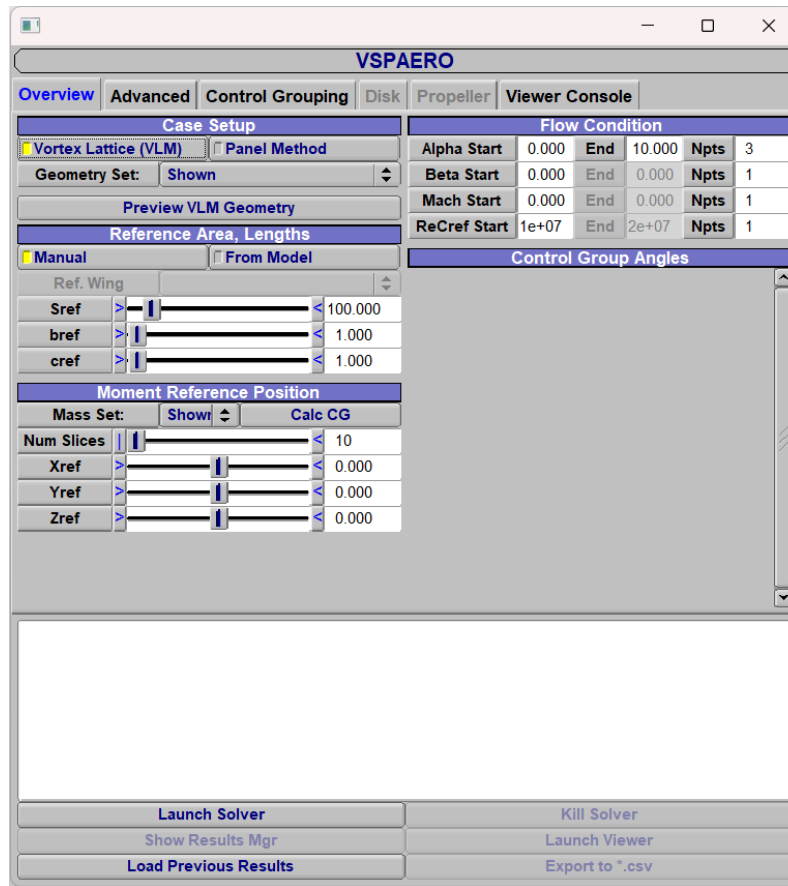


Figure 4.2 VSPAERO-Overview tab.

It is important to note that DegenGeom will write all the components in a model unless you specify a geometry set. The degenerate geometry files for your selected set of components are written from OpenVSP either by choosing DegenGeom under the Analysis menu or by opening the VSPAERO GUI and clicking Launch Solver. VSPAERO recognizes the DegenGeom/Cart3D file by the name `modelname_DegenGeom.vspaero` if running the vortex lattice method and `modelname.vspaero` if running the panel method. The easiest way to generate a file from scratch for a new model is to open VSPAERO and once you select the Overview tab, you'll find several different sliders and inputs that will help you define a Setup file. Once each value is defined for the flow conditions to be analyzed, click the Launch Solver button to automatically generate the Setup file and run VSPAERO with the VLM setup. If you view the `.vspaero` file, you should see that most of the values have been written in, between these:

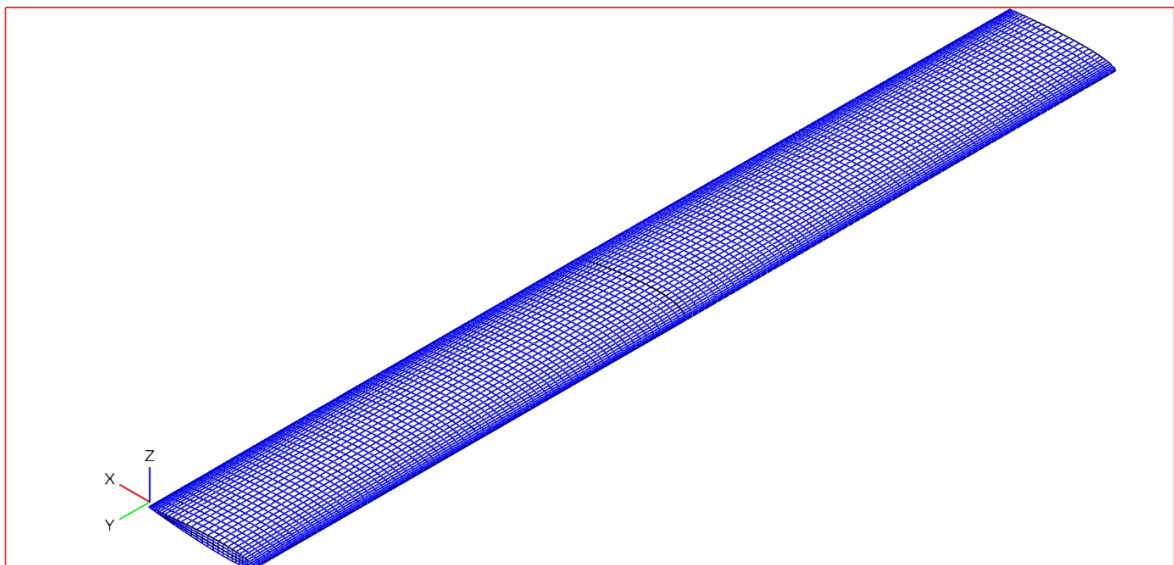
- The History file contains the integrated values as computed by VSPAERO for each iteration, we can find the lift coefficient, induced drag, force and moment coefficients, etc.

- The LOD file is a spanwise representation of the local lift, drag, and side force coefficients, this file is useful for the last vehicle plots.
- The ADB file, information about ADB here.
- The Stability File (STAB) contains the stability analysis output generated by the selection, in the Advanced tab, of one of these following sets: Stability, P Analysis, Q Analysis, R Analysis.
- The FEM file outputs the aerodynamic forces and moments for each span wise station in a wing section.

5. Geometry and study of the wing

5.1 Geometry

The first element to study is the Canadair CL-415 wing characterized by a rectangular geometry, wingspan of 28.6 m and a wing area of 100.33 m². Parameters entered in OpenVSP will not explicitly show units, so it is up to the user to enter the data in a way that is dimensionally consistent.



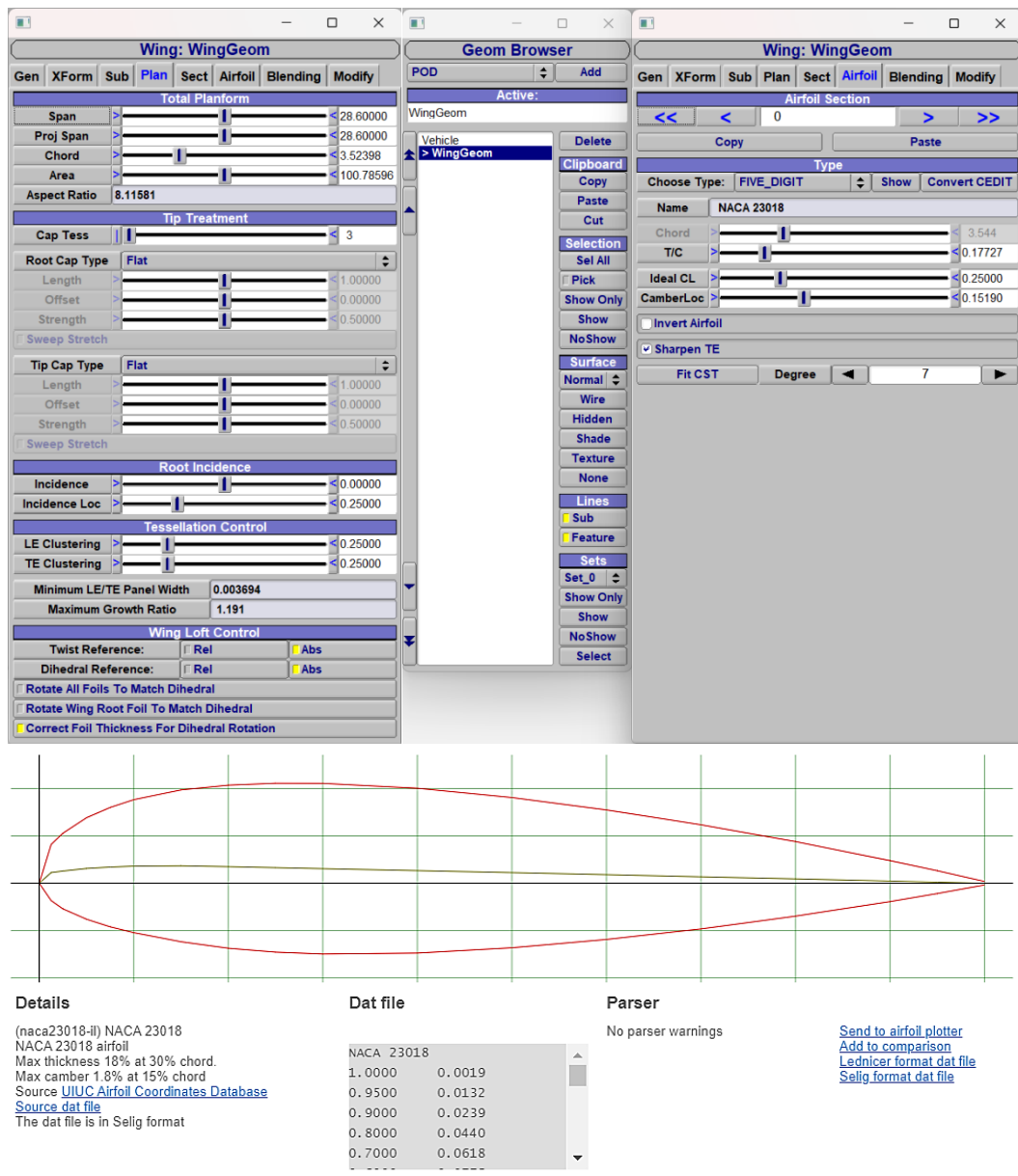


Figure 5.1 In the first image we have the wing (without sub-surfaces) visualized in OpenVSP, in the second the wing and profile parameters (plan and airfoil), in the last the NACA profile took from <http://airfoiltools.com>.

The NACA Five-Digit Series uses the same thickness forms as the Four-Digit Series, but the mean camber line is defined differently and the naming convention is a bit more complex. The first digit, when multiplied by $3/2$, yields the design lift coefficient (c_l) in tenths. The next two digits, when divided by 2, give the position of the maximum camber (p) in tenths of chord. The

final two digits again indicate the maximum thickness (t) in percentage of chord. For example, the NACA 23012 has a maximum thickness of 12%, a design lift coefficient of 0.3, and a maximum camber located 15% back from the leading edge. In this case the selected profile is NACA 23018.

5.2 Chordwise and Spanwise Refinement

It is now time to proceed with the study of the wing grid. This discussion will be organized in two parts: Chordwise Refinement and Spanwise Refinement. In both cases, the result to be achieved relates to that pair of values U and W such that the coefficient curves, obtained by varying Num_W and fixing Num_U (and vice versa), reach an asymptotic trend (at fixed angle of attack, $\alpha = 6^\circ$). The first case to consider is the Chordwise case in which the Num_W varies through the Gen tab of the Wing Geometry window.

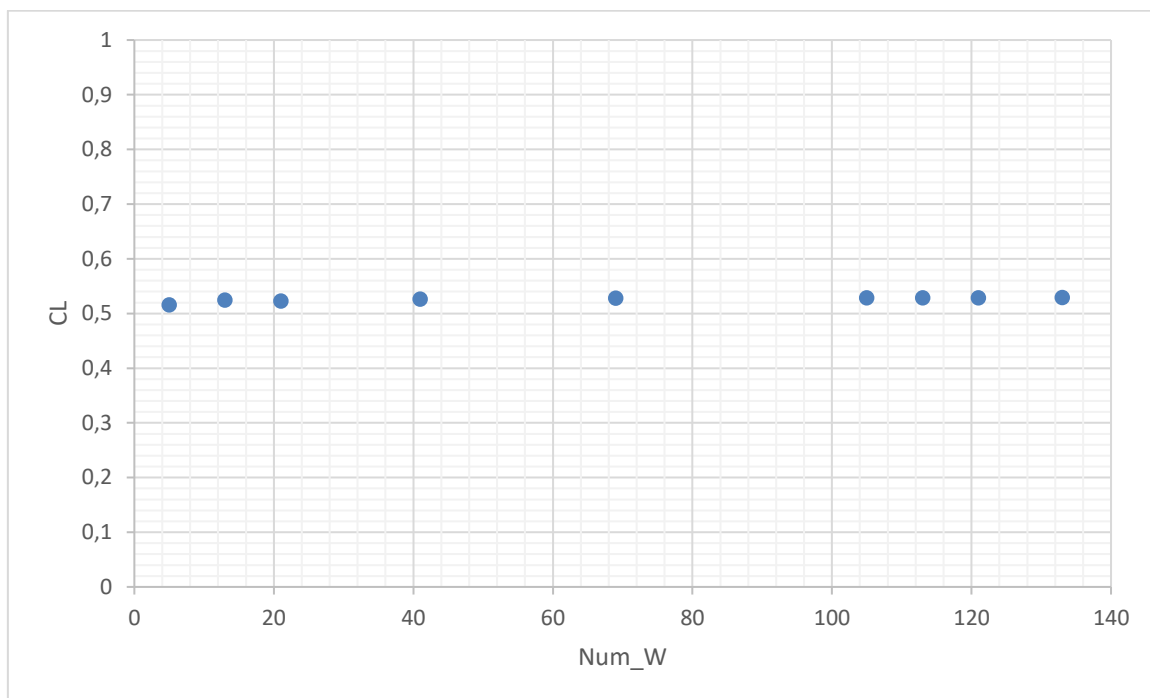


Figure 5.2 CL vs Num_W, $\alpha = 6^\circ$.

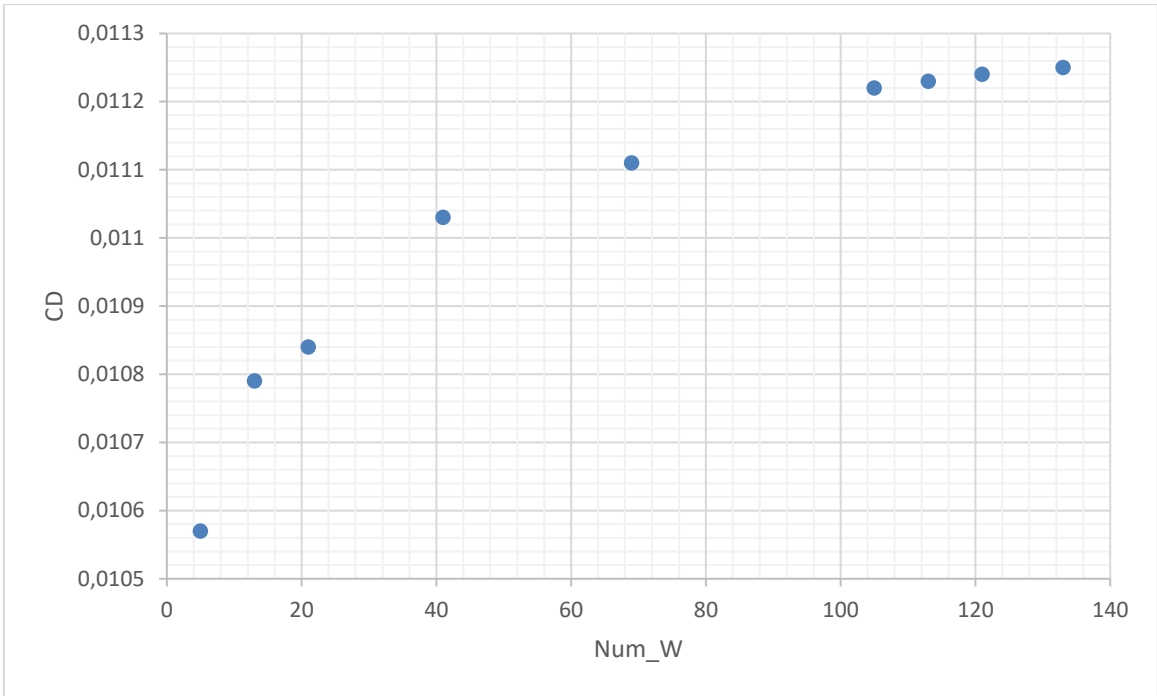


Figure 5.3 CD vs Num_W , $\alpha = 6^\circ$.

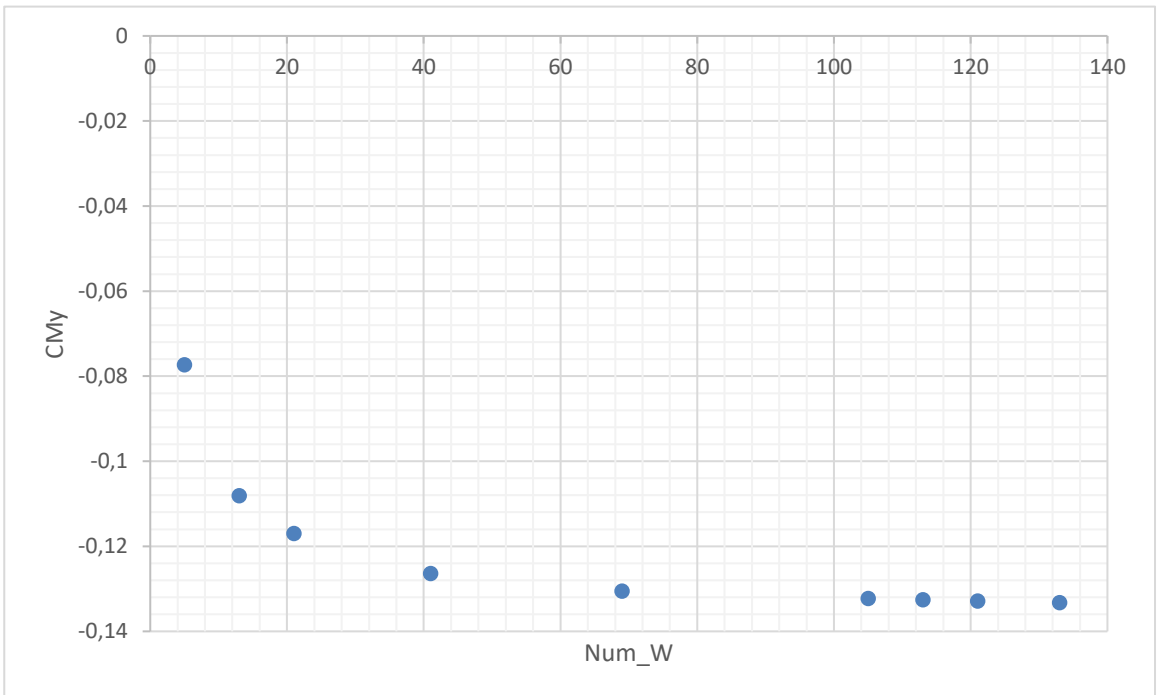


Figure 5.4 CM_y vs Num_W , $\alpha = 6^\circ$.

Making use of the previous premise an optimal value $Num_W \approx 69$ can be deduced from the above graphs. The Spanwise Refinement can be done by adjusting the Num_U parameter in the Sect tab of the Wing Geometry window and assuming a fixed previous value of Num_W . With the spanwise refinement the expected asymptotic behavior is strongly visible, in addition it is worth to note that increasing Num_U has an extraordinarily strong influence on the solution time so this will also affect subsequent operation times.

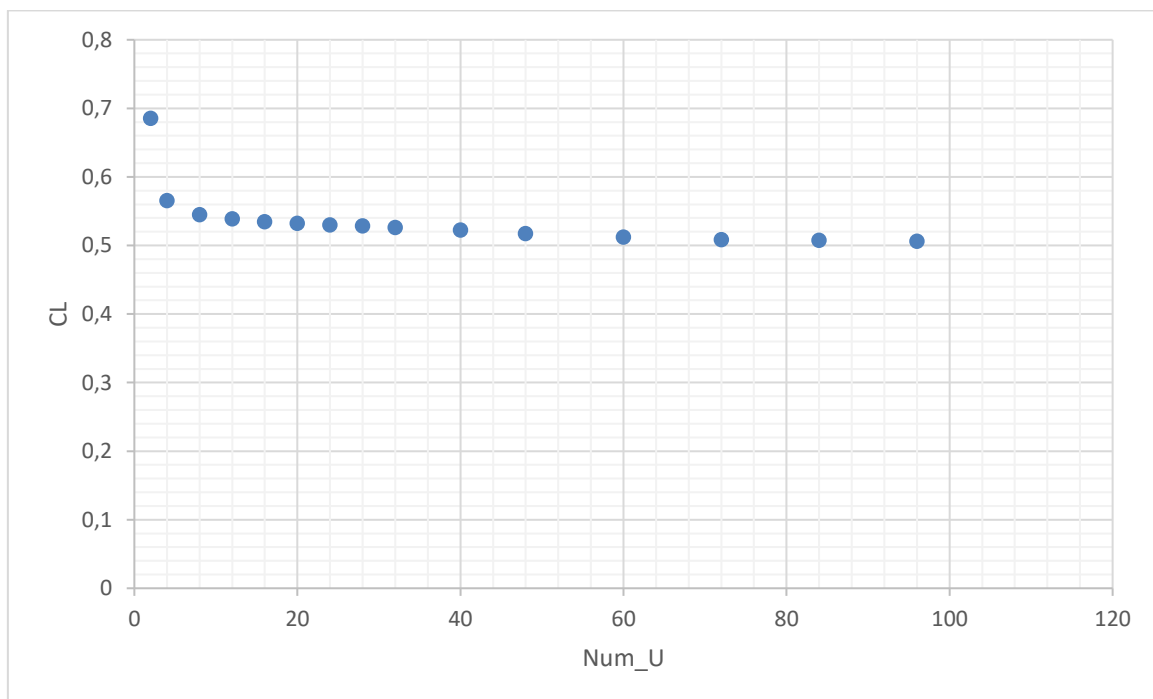


Figure 5.5 *CL vs Num_U, $\alpha = 6^\circ$.*

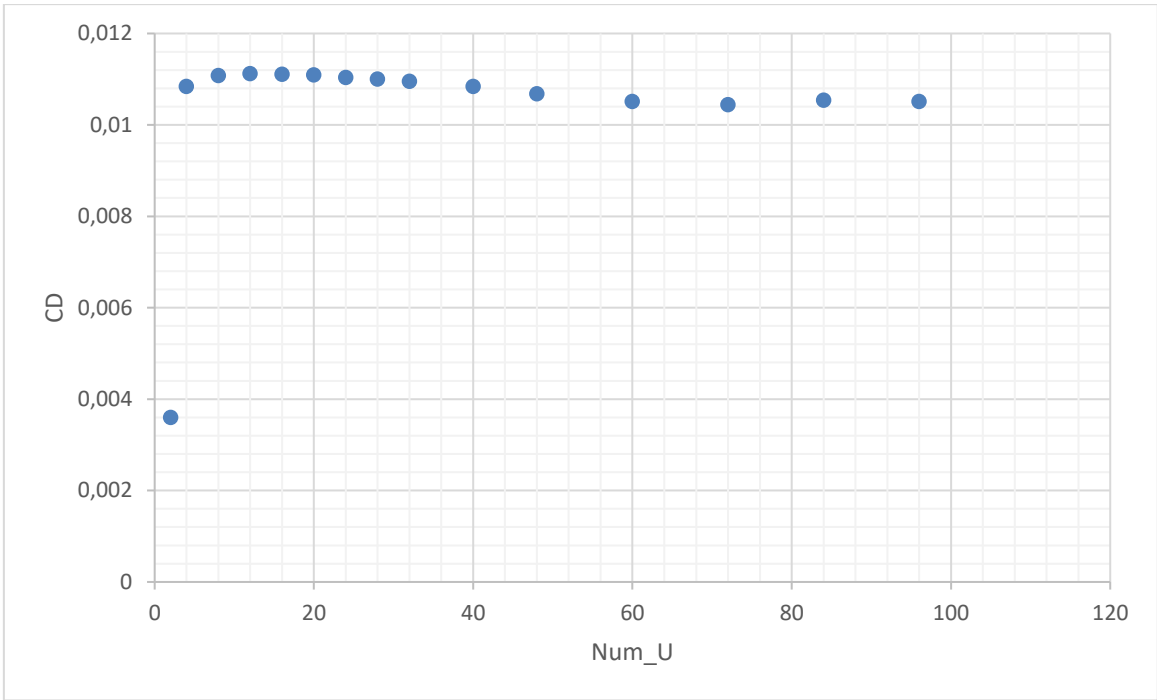


Figure 5.6 CD vs Num_U , $\alpha = 6^\circ$.

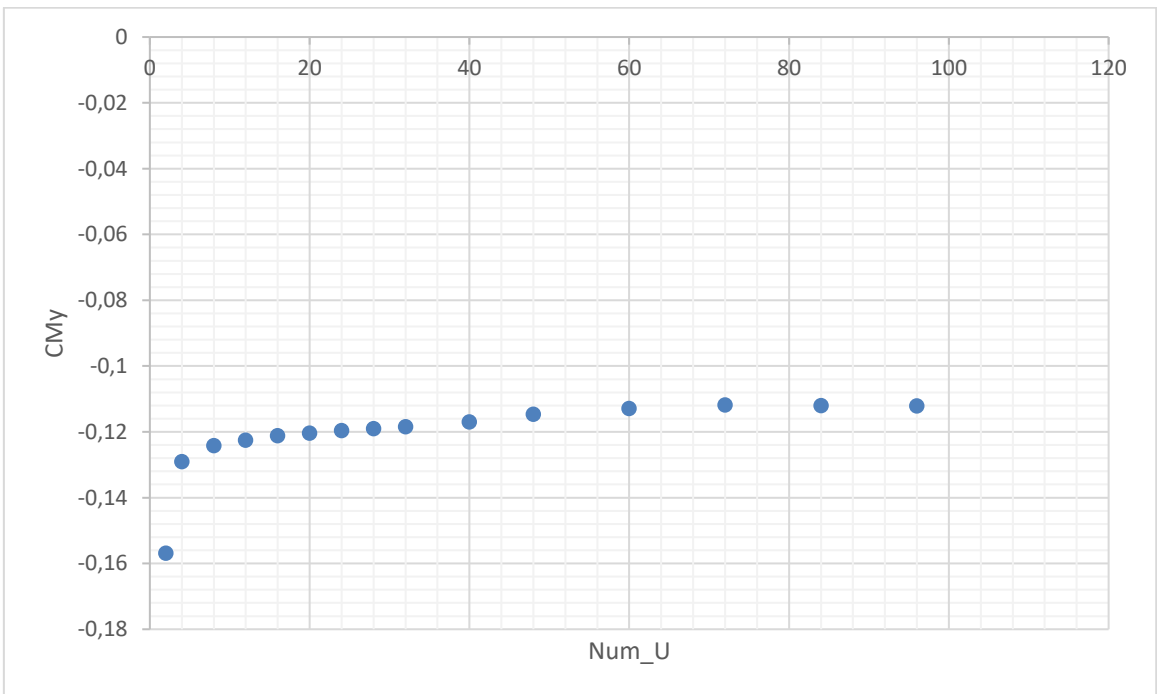


Figure 5.7 CM_y vs Num_U , $\alpha = 6^\circ$.

The asymptotic behavior is assumed in such graphs for $\text{Num_U} = 70$, with this value it is possible to identify the pair of values Num_W and Num_U that are fundamental for the purpose of creating the grid; thus summarizing: $\text{Num_W} = 69$ and $\text{Num_U} = 70$. The same grid will be adopted for the horizontal tailplane and the vertical tailplane, remembering that the prerogative is to focus on the load-bearing surfaces of the aircraft in order to be consistent with the way OpenVSP operates.

6. Geometry and study of the vehicle

6.1 Geometry modelling in OpenVSP

Figure 3.2 introduced the aircraft through the three basic views, which provide the geometric data based on which the aircraft was created on JPAD. Now it is possible to visualize the aircraft, having performed the export, on OpenVSP adding in addition the different control surfaces that will allow the user to perform stability analyses under different deflection conditions. Wing fences and auxiliary fins have been neglected in the following modeling.

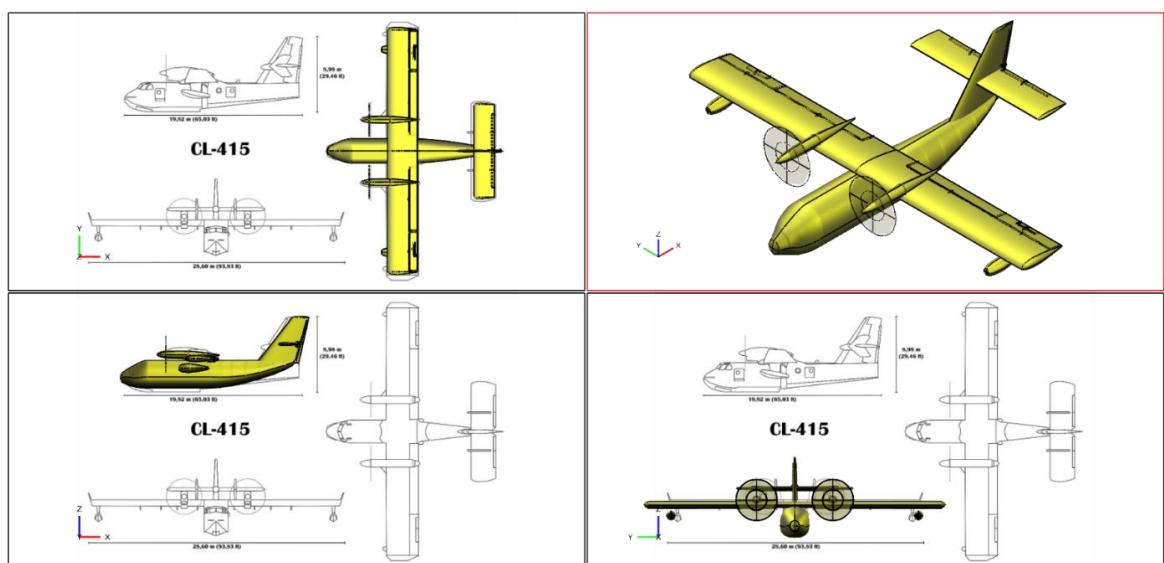


Figure 6.1 Aircraft visualized in OpenVSP (view comparison).

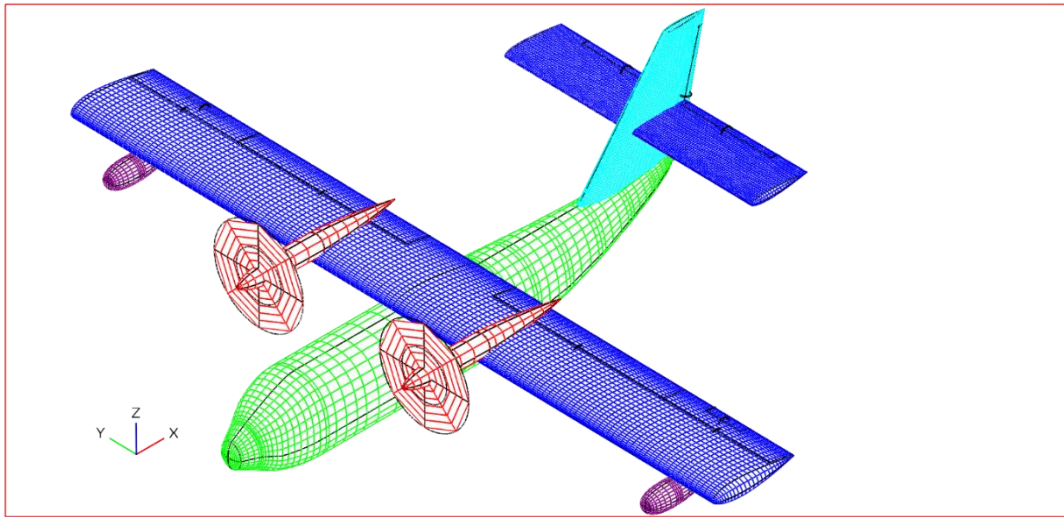
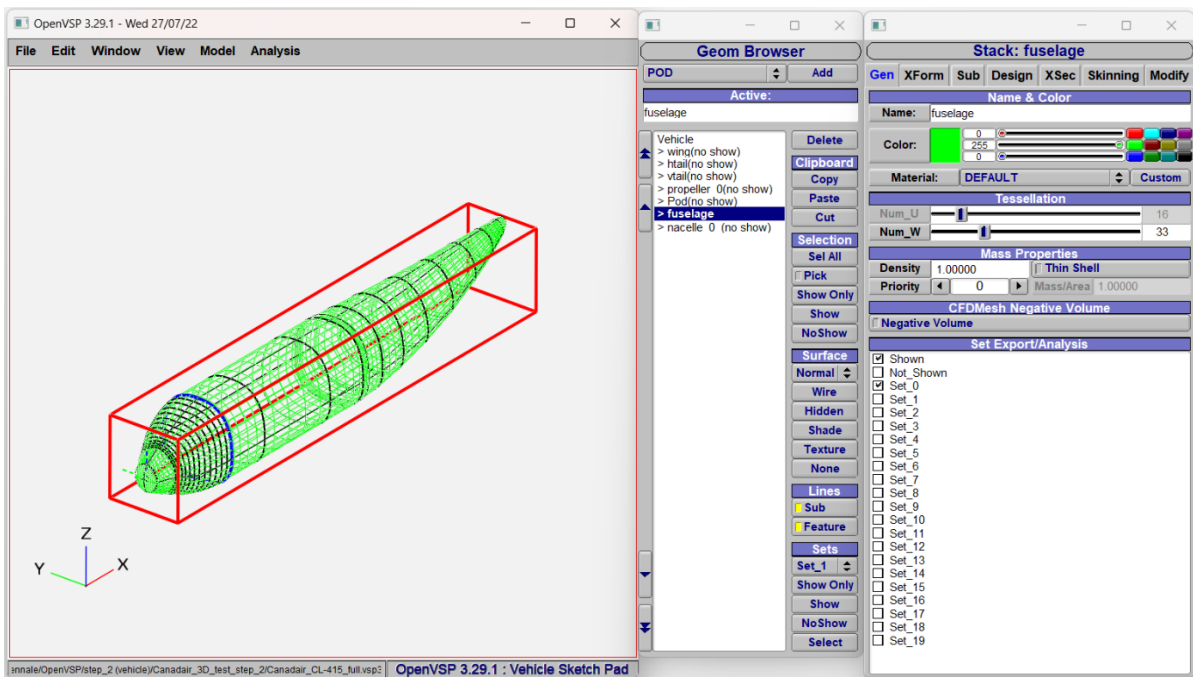


Figure 6.2 Aircraft visualized in OpenVSP (Surface “Hidden”).

The first element modified is the fuselage so below are tables with the parameters used for some section of the fuselage to model the fuselage design.



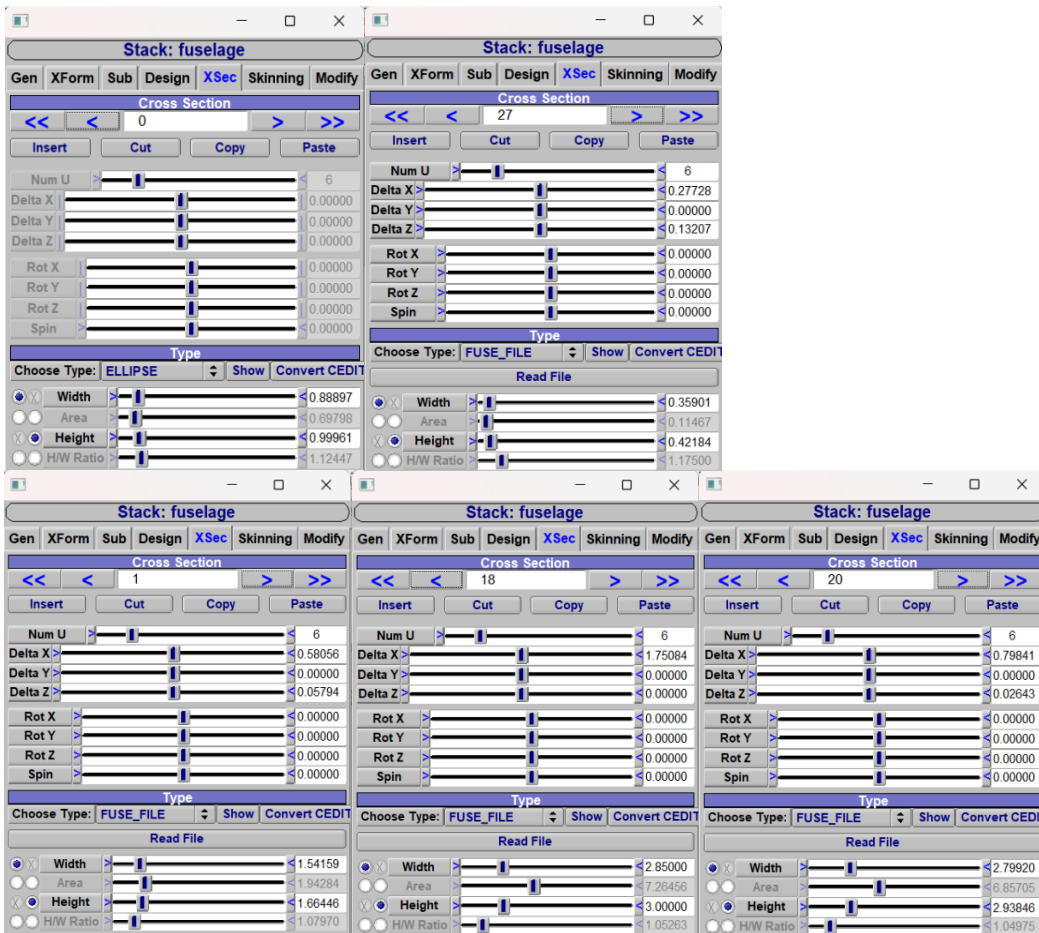


Figure 6.3 Gen and XSec panels for fuselage sections.

As already anticipated the grids used for the horizontal and vertical planes are the same as those used for the wing, for both it is considered a symmetrical airfoil NACA0012. Below are windows showing the geometric parameters for each of the planes shown.

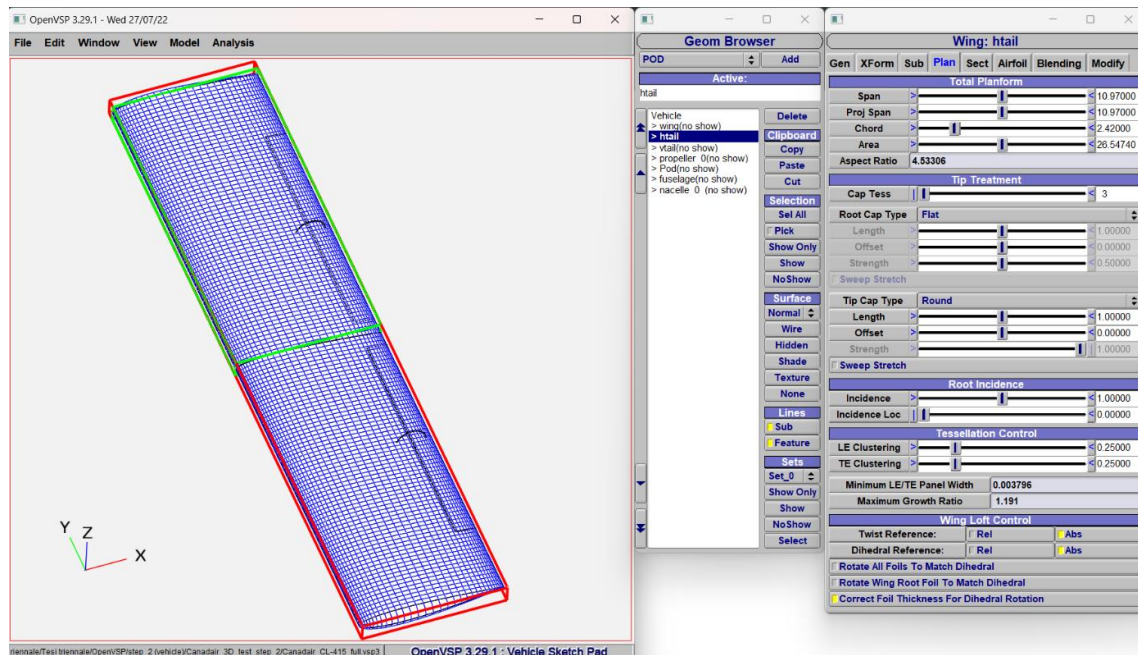


Figure 6.4 Plan panel for horizontal tail.

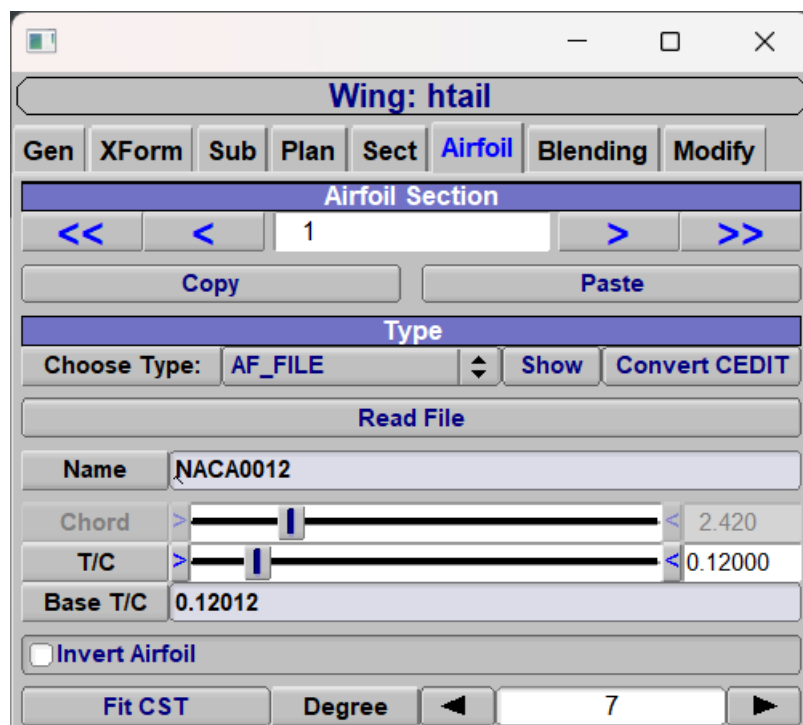


Figure 6.5 Airfoil panel for horizontal tail.

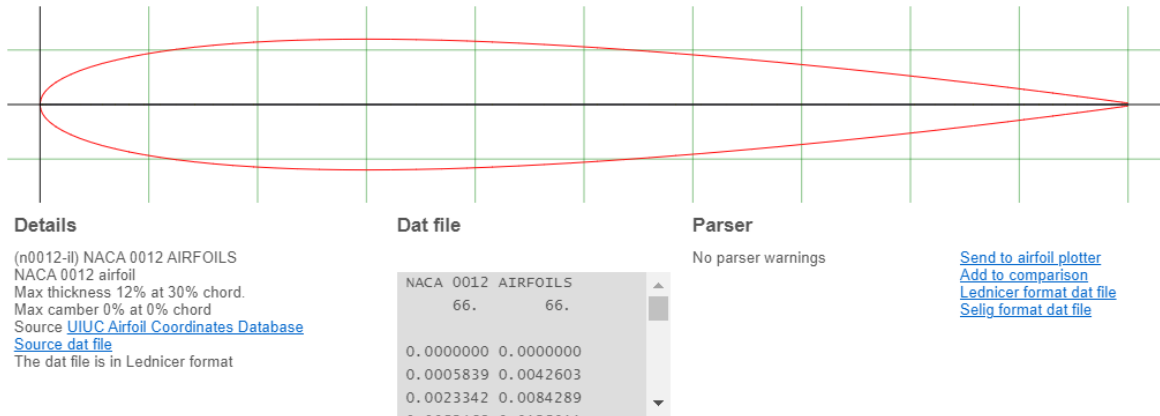


Figure 6.6 NACA 0012 profile took from <http://airfoiltools.com>.

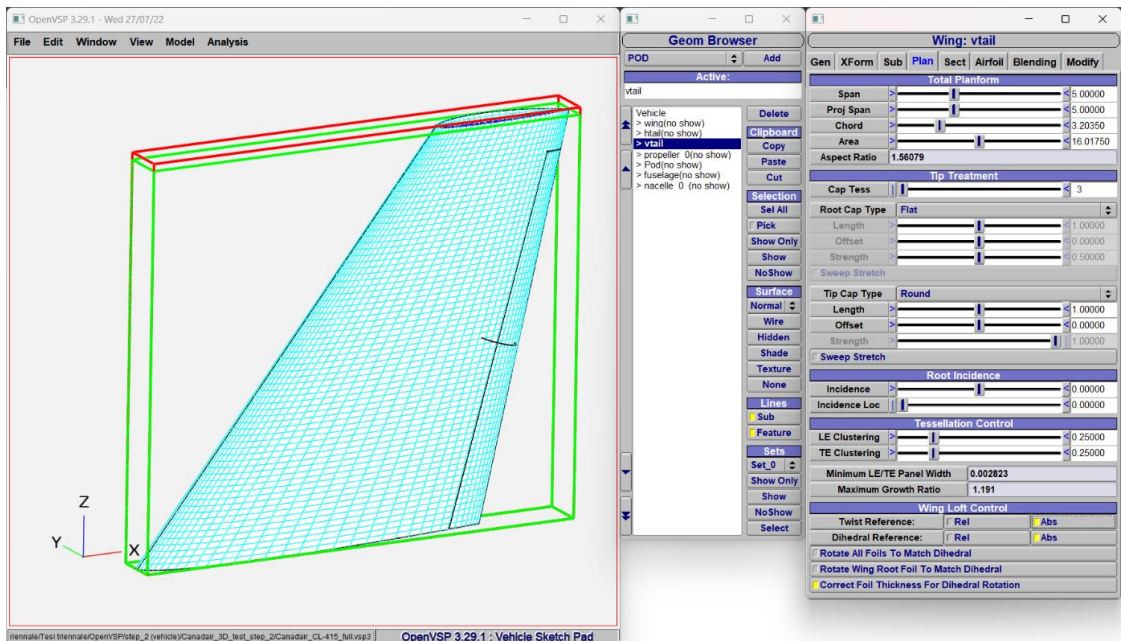


Figure 6.7 Plan panel for vertical tail.

Therefore, it is important to treat, based on the above action of the aircraft, the last components such as nacelles, propellers and pods.

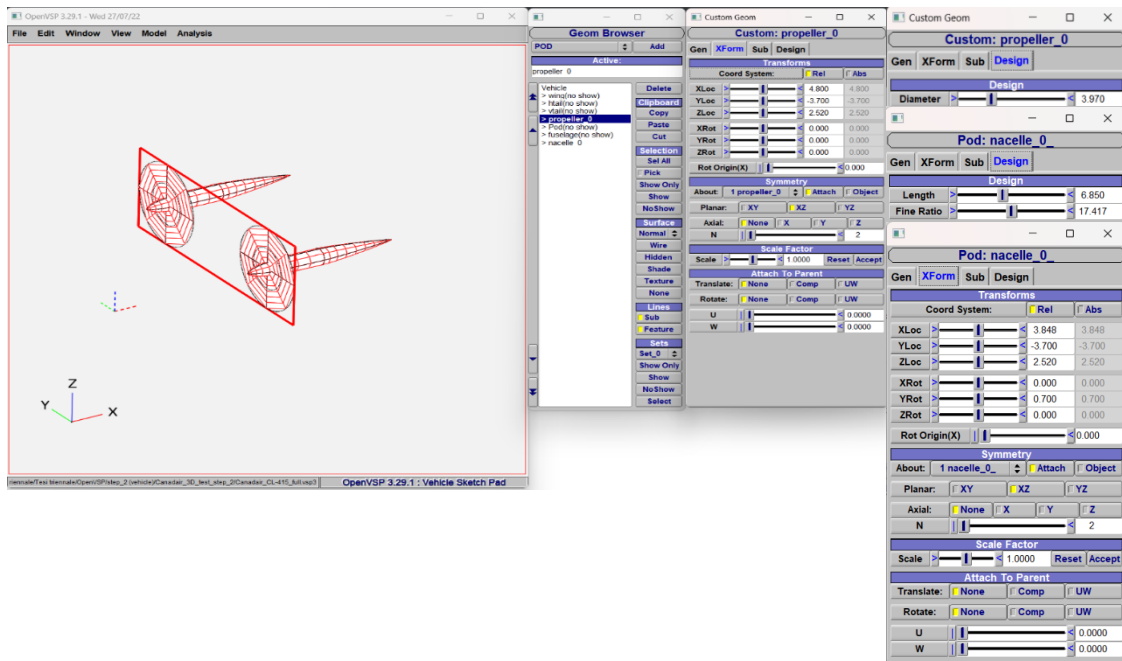


Figure 6.8 XForm and Design panel for nacelle and propeller.

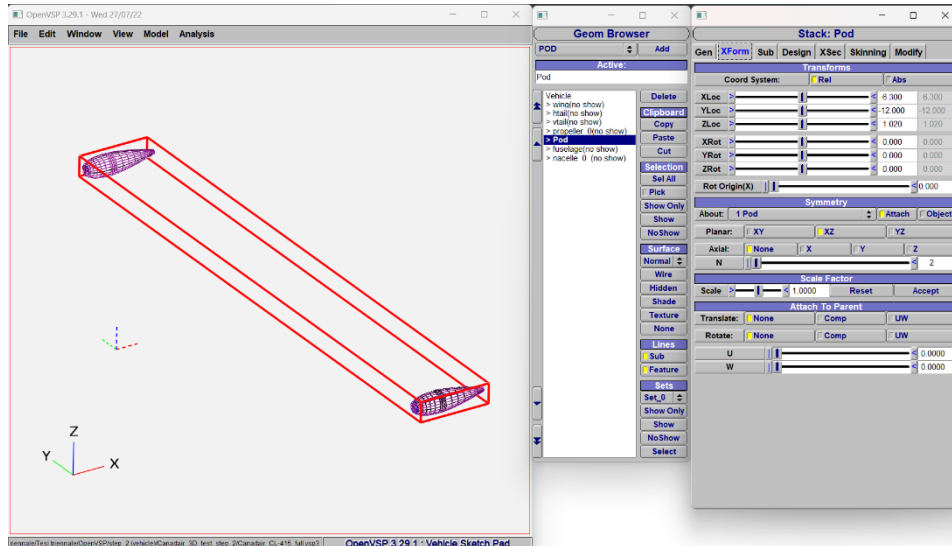


Figure 6.9 XForm panel for pod.

Referring again to the previously illustrated surfaces to complete the geometry of the aircraft it is necessary to add the control surfaces; these were added for the wings (flaps, aileron, aileron's

trim tab), the horizontal tail (elevator), the vertical tail (rudder). The aircraft is fitted with a powered rudder, ailerons and elevators. The control surfaces of the tail unit are constructed of honeycomb panels and the surface of the tail is aluminum alloy sheet.

Wing: wing

Gen XForm Sub Plan Sect Airfoil Blending Modify

Sub-Surface List

NAME	TYPE	SURF
Flap	Control Surf	Surf_0
TrimAileron	Control_Surf	Surf_0
Aileron	Control_Surf	Surf_0

Delete

Type Line ▲▼

Surface Surf_0 ▲▼

Add

Wing: htail

Gen XForm Sub Plan Sect Airfoil Blending Modify

Sub-Surface List

NAME	TYPE	SURF
Elevator	Control Surf	Surf_0

Delete

Type Line ▲▼

Surface Surf_0 ▲▼

Add

Wing: vtail
Gen XForm Sub Plan Sect Airfoil Blending Modify
Sub-Surface List**Delete**
Type Line ▲▼
Surface Surf_0 ▲▼
Add

Figure 6.10 Sub panel for: wing, horizontal tail and vertical tail.

6.2 Results and discussion

With the help of VSPAERO module, analysis was performed choosing Vortex Lattice (VLM) as the **Case setup**, **References Area and lengths** were deduced From Model, for Moment Reference Position a **number of slices** equal to 10 (default) was chosen. The **Flow Conditions** were modified to have 4 values of Alpha Start from 0° up to 10°, Beta Start constantly null, Mach fixed at 0.001 and Reynolds number fixed at 5e+06.

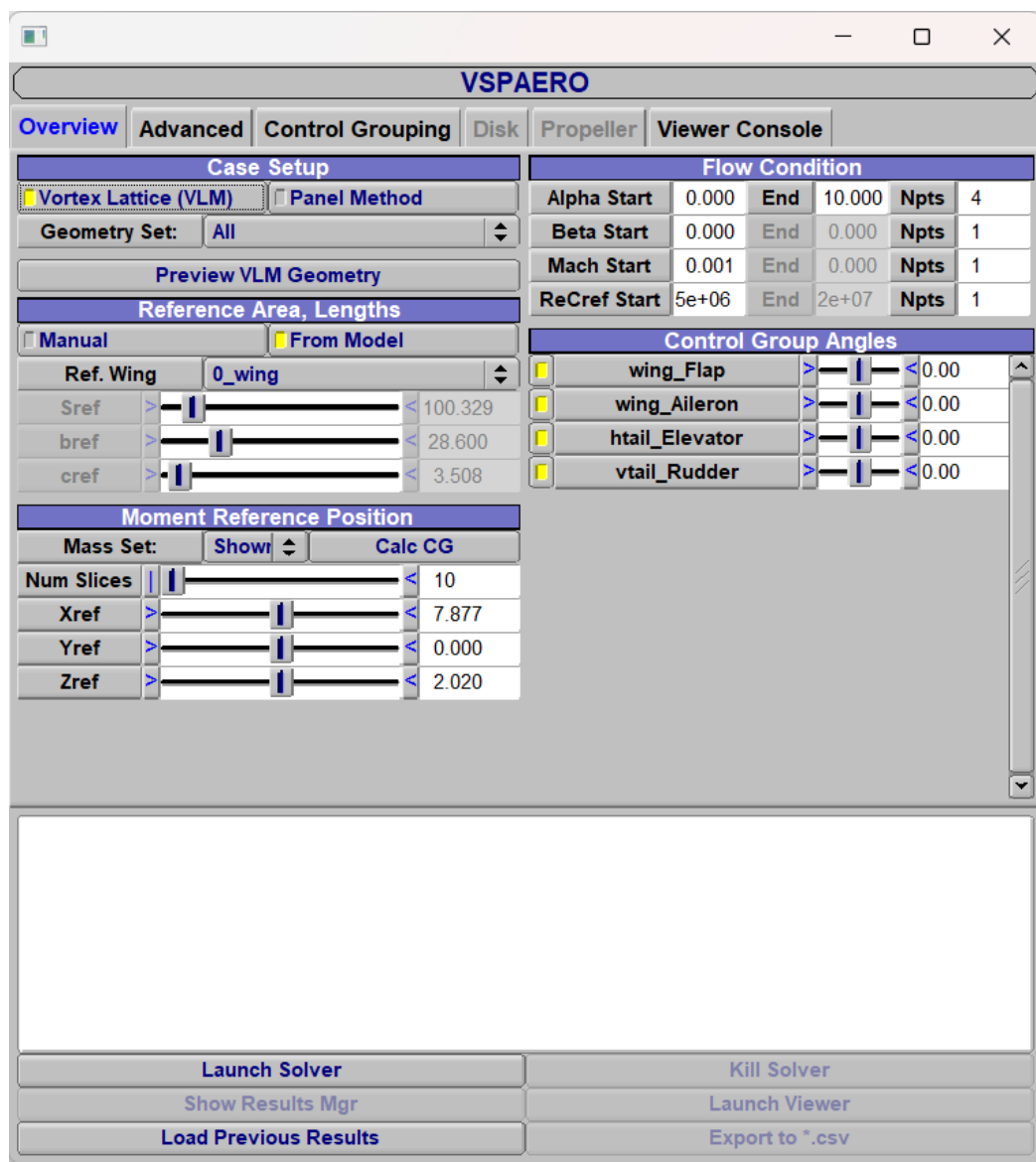


Figure 6.11 VSPAERO Overview panel.

With the **Control Group Angles** panel the flap deflection is modified considering control surfaces all at 0° , in fact the angles chosen for the deflections are 0° , 15° , 30° . It is possible to show the results of the analysis obtained from the inputs immitted in the previous panel through summary tables and graphs, similarly to what was done in the section on wing analysis.

AoA	CL	CDtot	L/D	CMy
0,0	0,10	0,0173	5,8	-0,051
3,3	0,40	0,0251	16,1	-0,130
6,7	0,71	0,0423	16,7	-0,209
10,0	1,00	0,0687	14,6	-0,288

Table 6.1 Table of coefficients, flap= 0° .

AoA	CL	CDtot	L/D	CMy
0,0	0,52	0,0351	14,7	-0,039
3,3	0,82	0,0530	15,4	-0,122
6,7	1,11	0,0798	14,0	-0,208
10,0	1,40	0,1144	12,3	-0,279

Table 6.2 Table of coefficients, flap= 15° .

AoA	CL	CDtot	L/D	CMy
0,0	0,83	0,0668	12,4	-0,029
3,3	1,12	0,0908	12,3	-0,114
6,7	1,41	0,1231	11,5	-0,207
10,0	1,69	0,1625	10,4	-0,281

Table 6.3 Table of coefficients, flap= 30° .

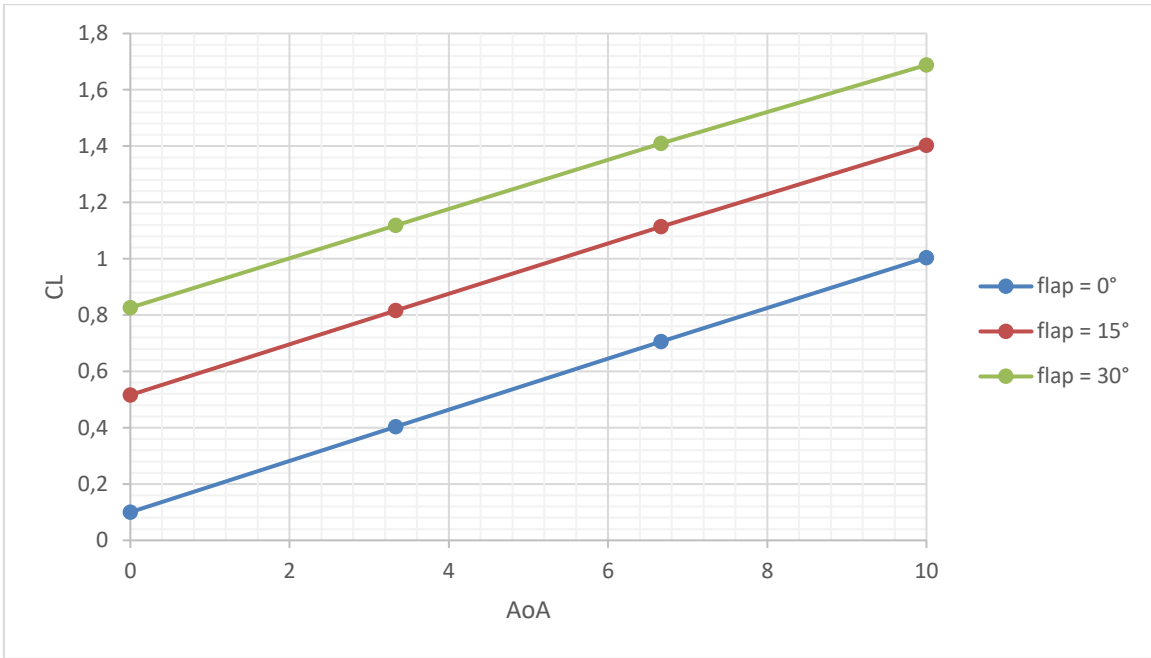


Figure 6.12 CL vs AoA plot as flap deflection changes.

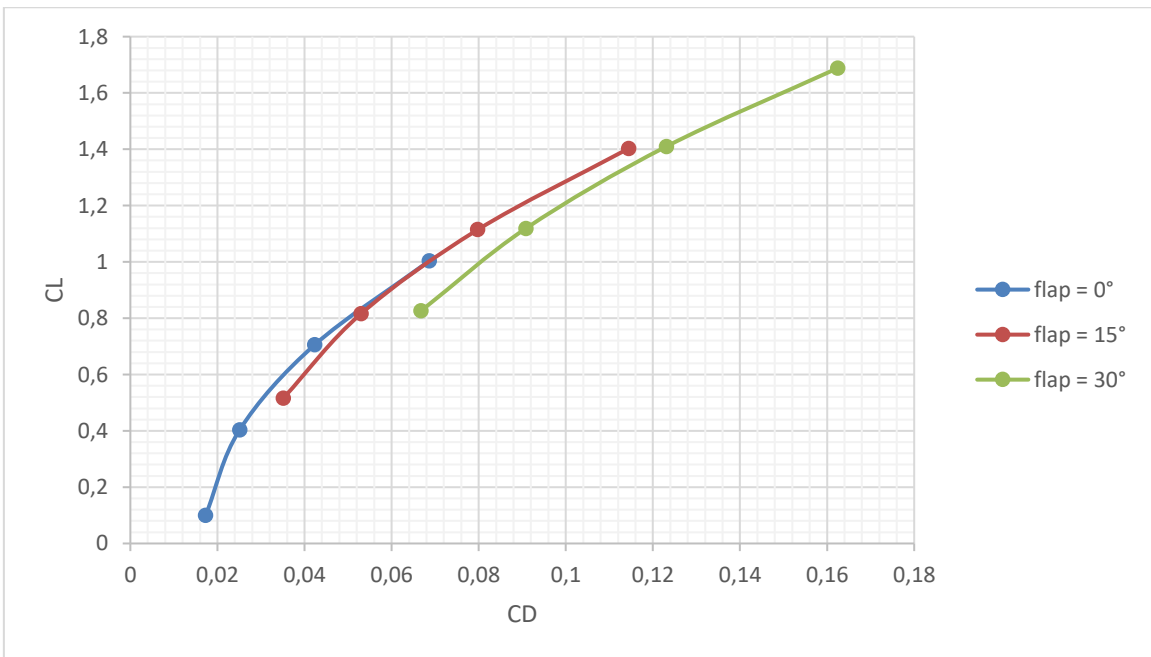


Figure 6.13 CL vs CD plot as flap deflection changes.

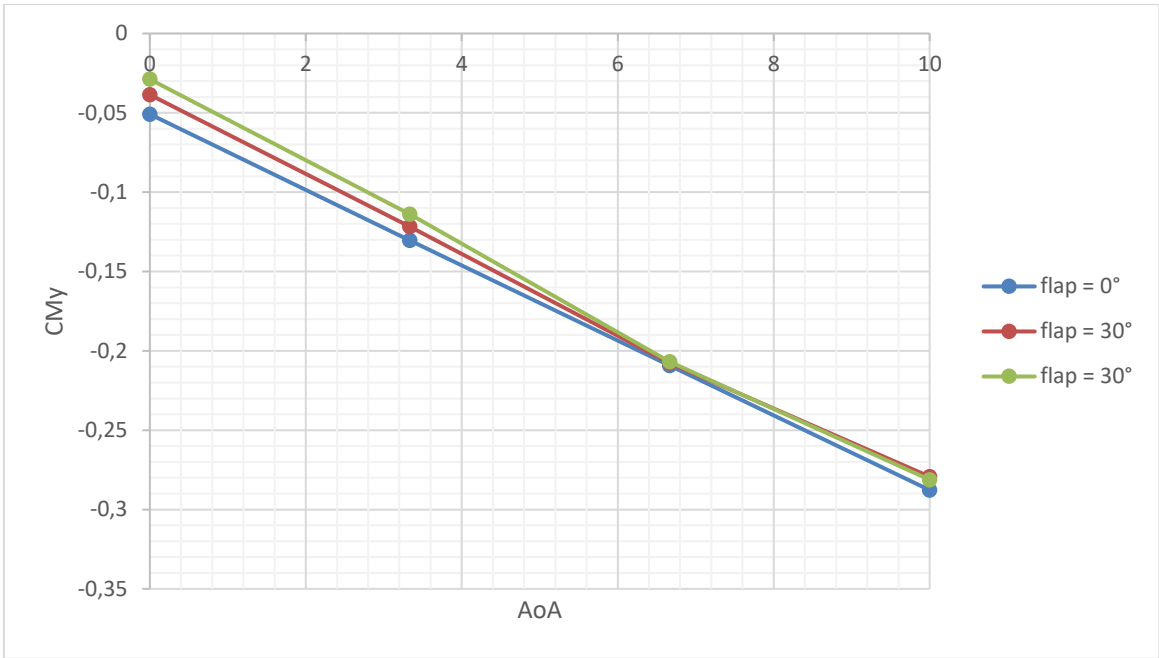


Figure 6.14 CM_y vs AoA plot as flap deflection changes, Vehicle CG (7.88,0,2.02).

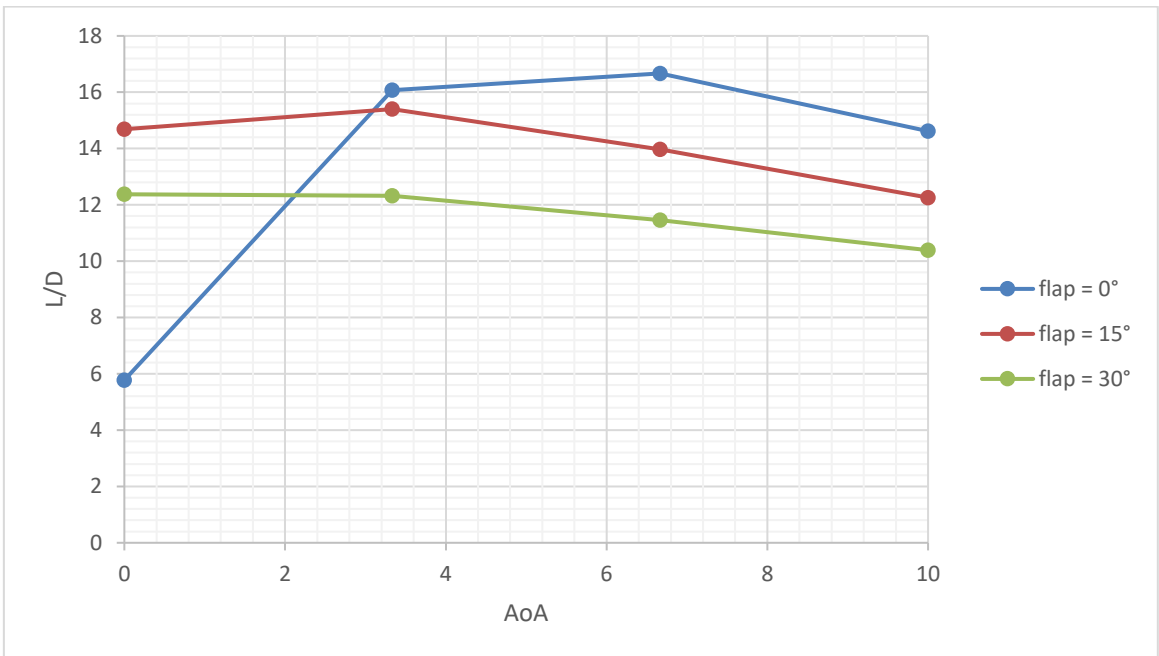


Figure 6.15 L/D vs AoA plot as flap deflection changes.

Once the process is finished there is an opportunity to view the results obtained on the aircraft with "Plate Degen" geometry by changing the Solution Case.

VSPAERO Viewer, flap = 0°

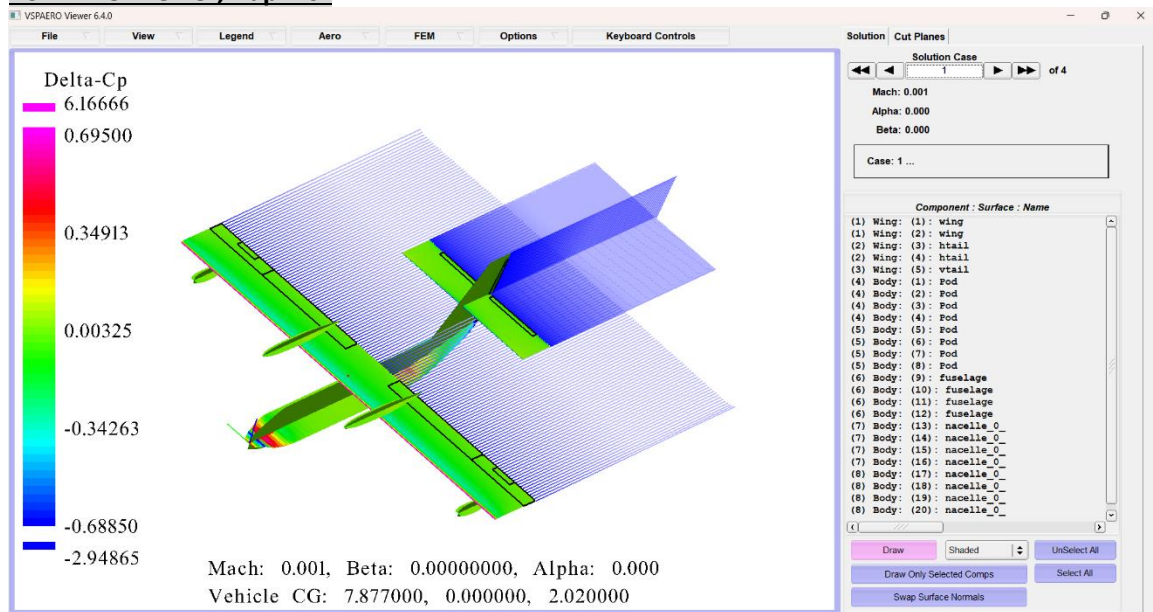


Figure 6.16 Solution Case 1, flap=0°, Alpha = 0

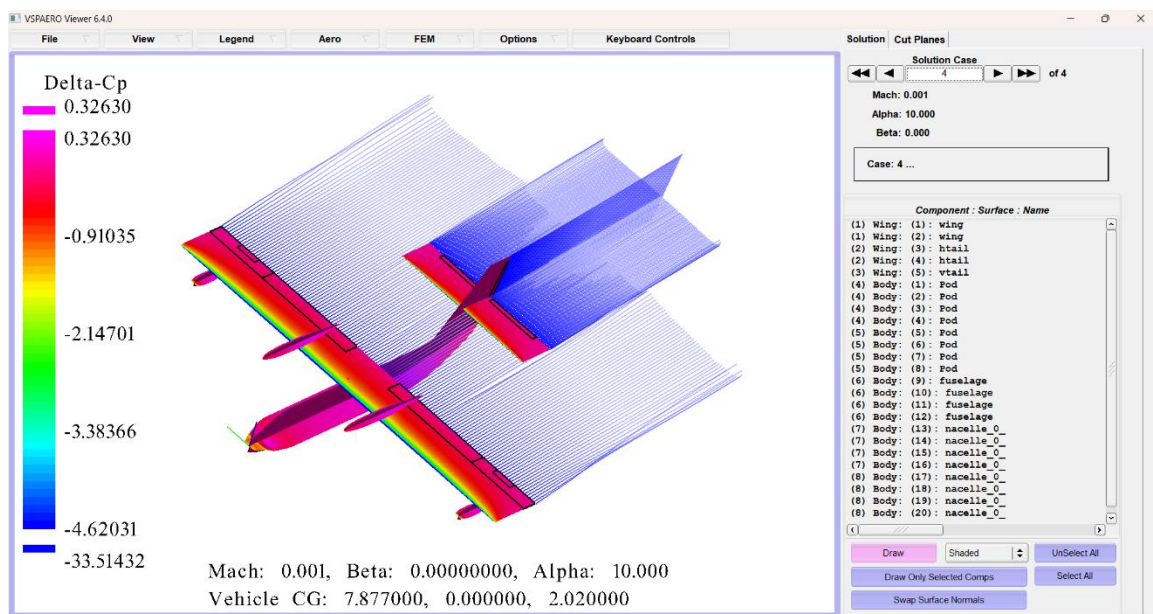


Figure 6.17 Solution Case 4, flap=0°, Alpha = 10°.

VSPAERO Viewer, flap = 15°

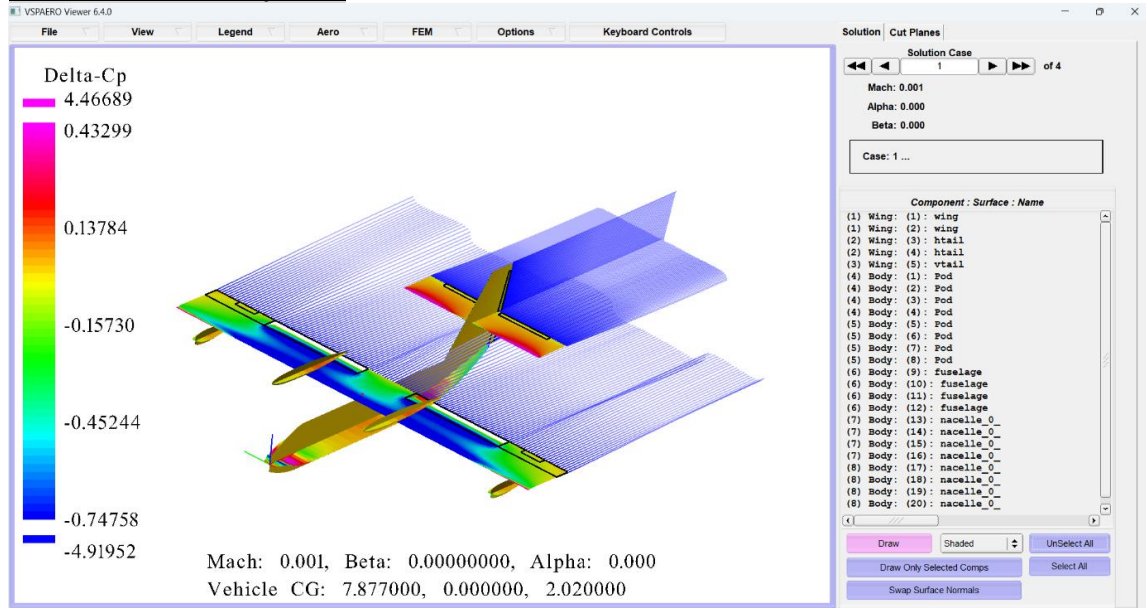


Figure 6.18 Solution Case 1, flap=15°, Alpha = 0°.

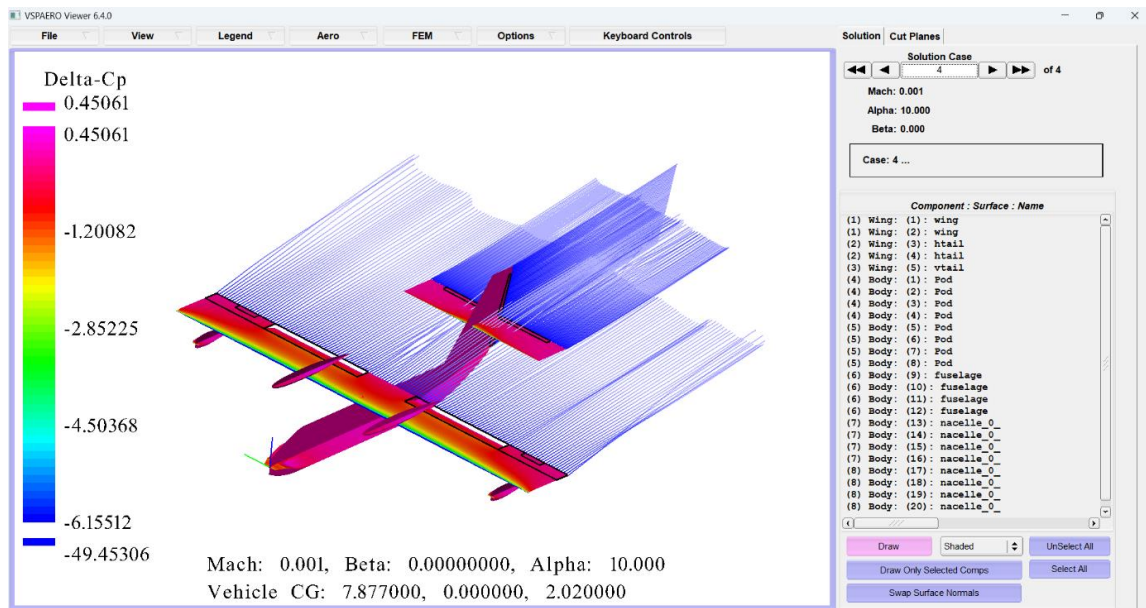


Figure 6.19 Solution Case 4, flap=15°, Alpha = 10°.

VSPAERO Viewer, flap = 30°

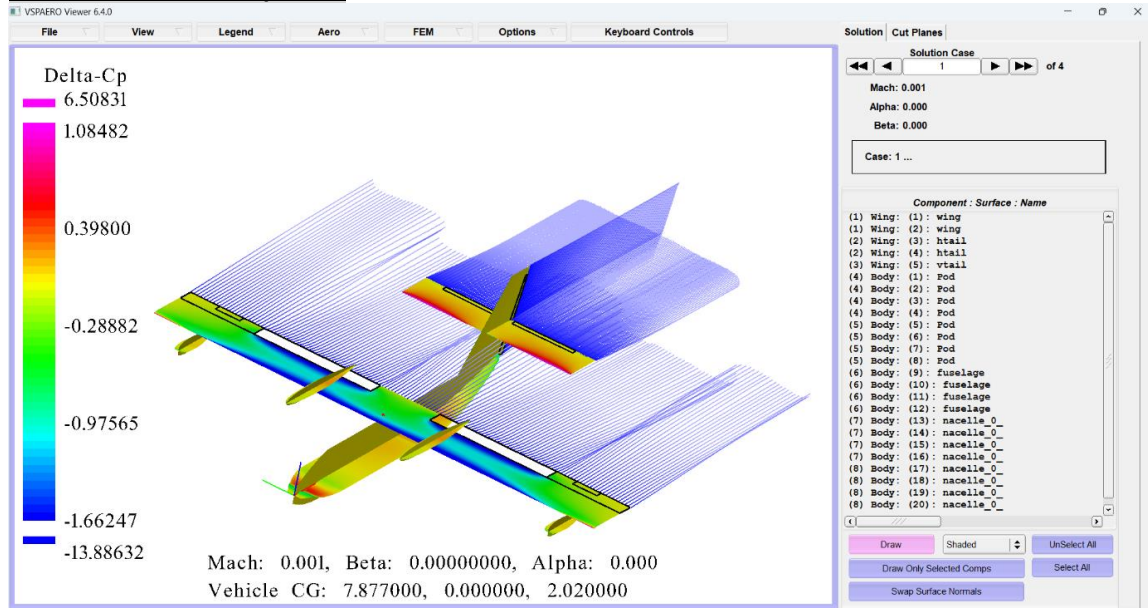


Figure 6.20 Solution Case 1, flap=30°, Alpha = 0°.

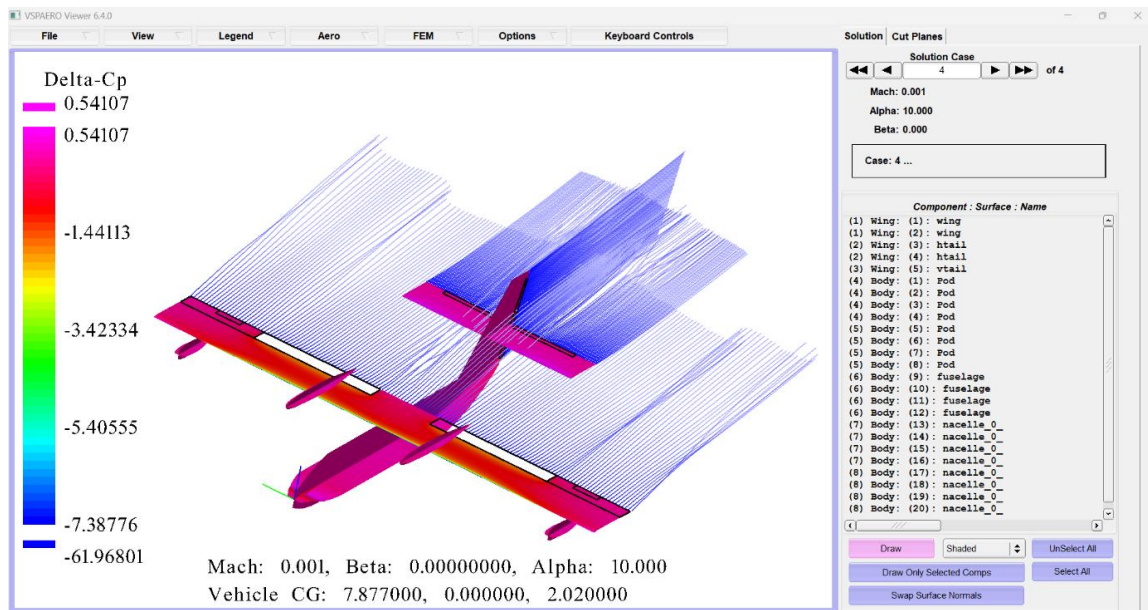


Figure 6.21 Solution Case 4, flap=30°, Alpha = 10°.

To find the neutral stability condition, it is necessary to calculate the neutral point. The first thing to do is to start from linearizing the aircraft pitching moment coefficient and set the equation related to $C_{M\alpha}$ equal to zero:

$$C_{M\alpha} = C_{L\alpha,W} \cdot (\bar{x}_G - \bar{x}_{ac,WB}) - \eta_H \cdot \frac{S_H}{S} \cdot (\bar{x}_{ac,H} - \bar{x}_G) \cdot C_{L\alpha,H} \cdot \left[1 - \left(\frac{d\epsilon}{d\alpha} \right)_H \right] = 0$$

At this point it is possible to pull out the neutral point expression remembering that when $\bar{x}_G = \bar{x}_N$ the airplane's equilibrium in pitch is neutrally stable. Additionally, assuming $C_{L\alpha,WB} = C_{L\alpha,W}$:

$$\bar{x}_N \stackrel{\text{def}}{=} \frac{x_N}{\bar{c}} = \frac{\bar{x}_{ac,WB} + \eta_H \cdot \frac{C_{L\alpha,H}}{C_{L\alpha,WB}} \cdot \frac{S_H}{S} \cdot \bar{x}_{ac,H} \cdot \left[1 - \left(\frac{d\epsilon}{d\alpha} \right)_H \right]}{1 + \eta_H \cdot \frac{C_{L\alpha,H}}{C_{L\alpha,WB}} \cdot \frac{S_H}{S} \cdot \left[1 - \left(\frac{d\epsilon}{d\alpha} \right)_H \right]}$$

From the previous equation derives the definition of the static stability margin:

$$SM = \bar{x}_G - \bar{x}_N$$

Another useful form of $C_{M\alpha}$ is given by this simple equation:

$$C_{M\alpha} = C_{L\alpha} \cdot (\bar{x}_G - \bar{x}_N) = C_{L\alpha} \cdot SM$$

Thus, to have a stable aircraft one must deal with some usual conditions like $x_G < x_N$ i.e., $C_{M\alpha} < 0$ and $SM < 0$. Typically $SM \approx 0.10 \div 0.20$. By considering the horizontal tail volume ratio $\bar{V}_H = \frac{S_H}{S} \cdot \frac{l_H}{\bar{c}} = \frac{S_H}{S} \cdot (\bar{x}_{ac,H} - \bar{x}_G)$ independent from the CG position it is immediate to show an alternative neutral point equation:

$$\bar{x}_N \approx \bar{x}_{ac,WB} + \eta_H \cdot \frac{C_{L\alpha,H}}{C_{L\alpha,W}} \cdot \bar{V}_H \cdot \left[1 - \left(\frac{d\epsilon}{d\alpha} \right)_H \right]$$

By assuming the position of the X_G placed at 25% of the aerodynamic chord and using the above expressions it follows that:

SM	-0,262
xg	0,250
CM_alpha	-0,024
CL_alpha	0,091
Neutral point	0,512

Comparing those results with the previously ones represented on the plots of the full vehicle it is possible to see a small variation of the values of $C_{M\alpha}$ and $C_{L\alpha}$ compared to the parameters offered by the stability analysis (flap=0°):

	CL_alpha		CM_alpha
Excel	0,0904	Excel	-0,0237
STAB	0,0912	STAB	-0,0239

From the LOD file, the lift coefficient values can be extracted, which were related to the wing half-opening and the horizontal tailplane half-opening to obtain the dimensionless values to be put on the x-axis and subsequently plot the load distribution. To do this, the angle of attack was again set at 6.7°.

# Name	Value	Units
Sref_	100,3288	m^2
Cref_	3,508	m
Bref_	28,6	m
Xcg_	7,877	m
Ycg_	0	m
Zcg_	2,02	m
Mach_	0,001	no_unit
AoA_	6,7	deg
Beta_	0	deg
Rho_	1,225	kg/m
Vinf_	100	m/s
Roll__Rate	0	rad/s
Pitch_Rate	0	rad/s
Yaw___Rate	0	rad/s

Table 6.4 Overview Table, AoA=6.7°.

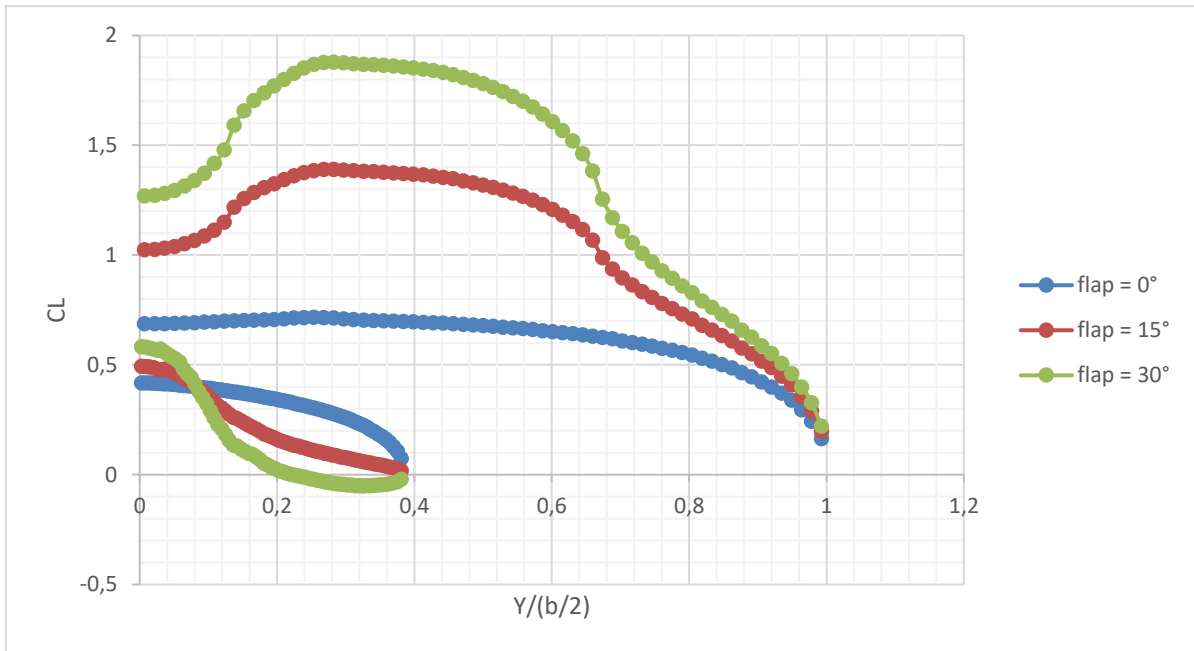


Figure 6.22 Load Distributions ranging with flap deflections. The lower curves refer to the tailplane. Note the downwash effect on the horizontal tail load due to the flap.

In those plots there is unmistakable evidence of the deflection marked by the depressions that intensify as flap deflection angle increases.

So, the last type of process that we discuss, managed by VSPAERO, is the stability analysis conducted around $\alpha=0^\circ$ and turning off flap deflections.

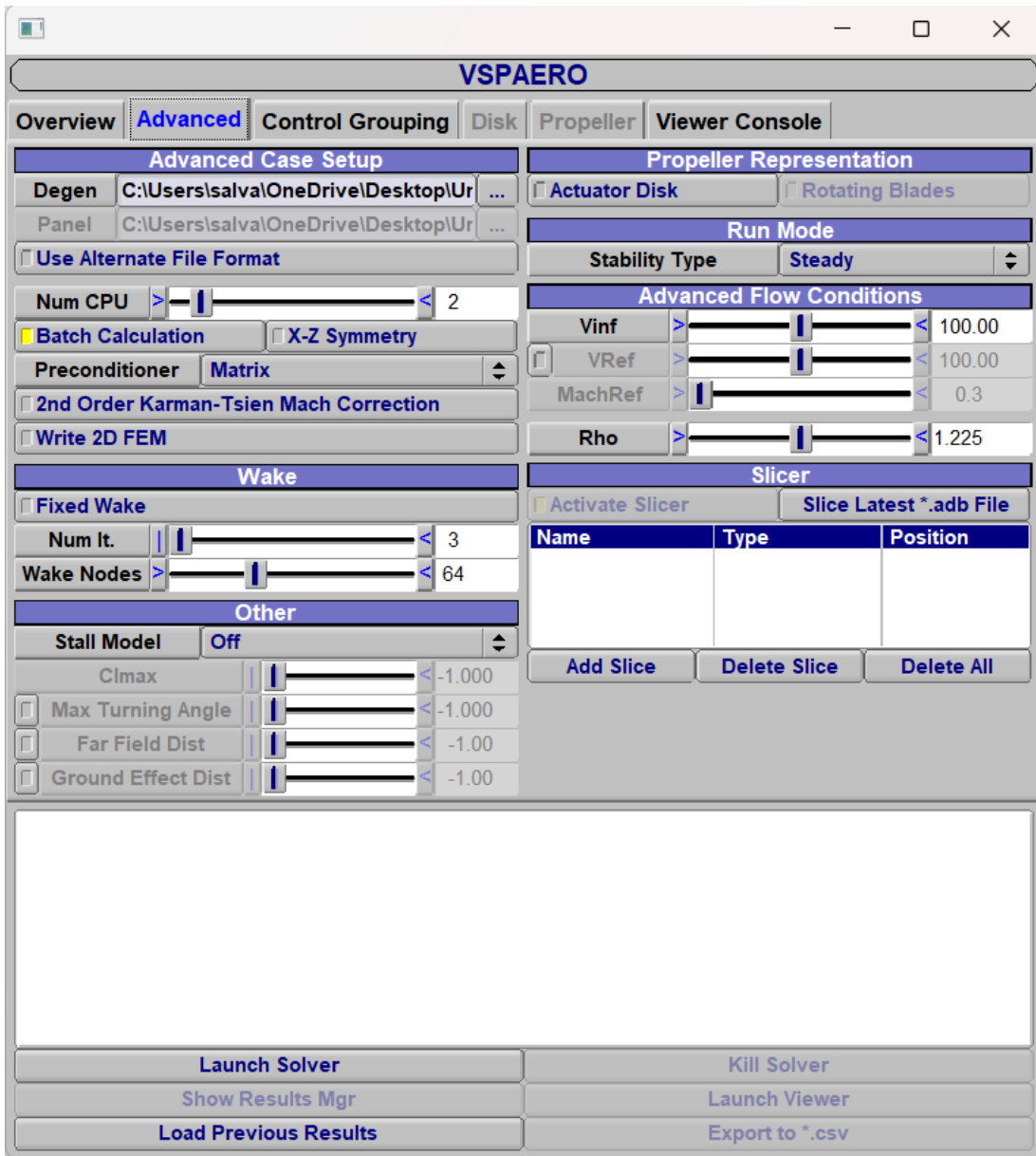


Figure 6.23 VSPAERO Advanced panel.

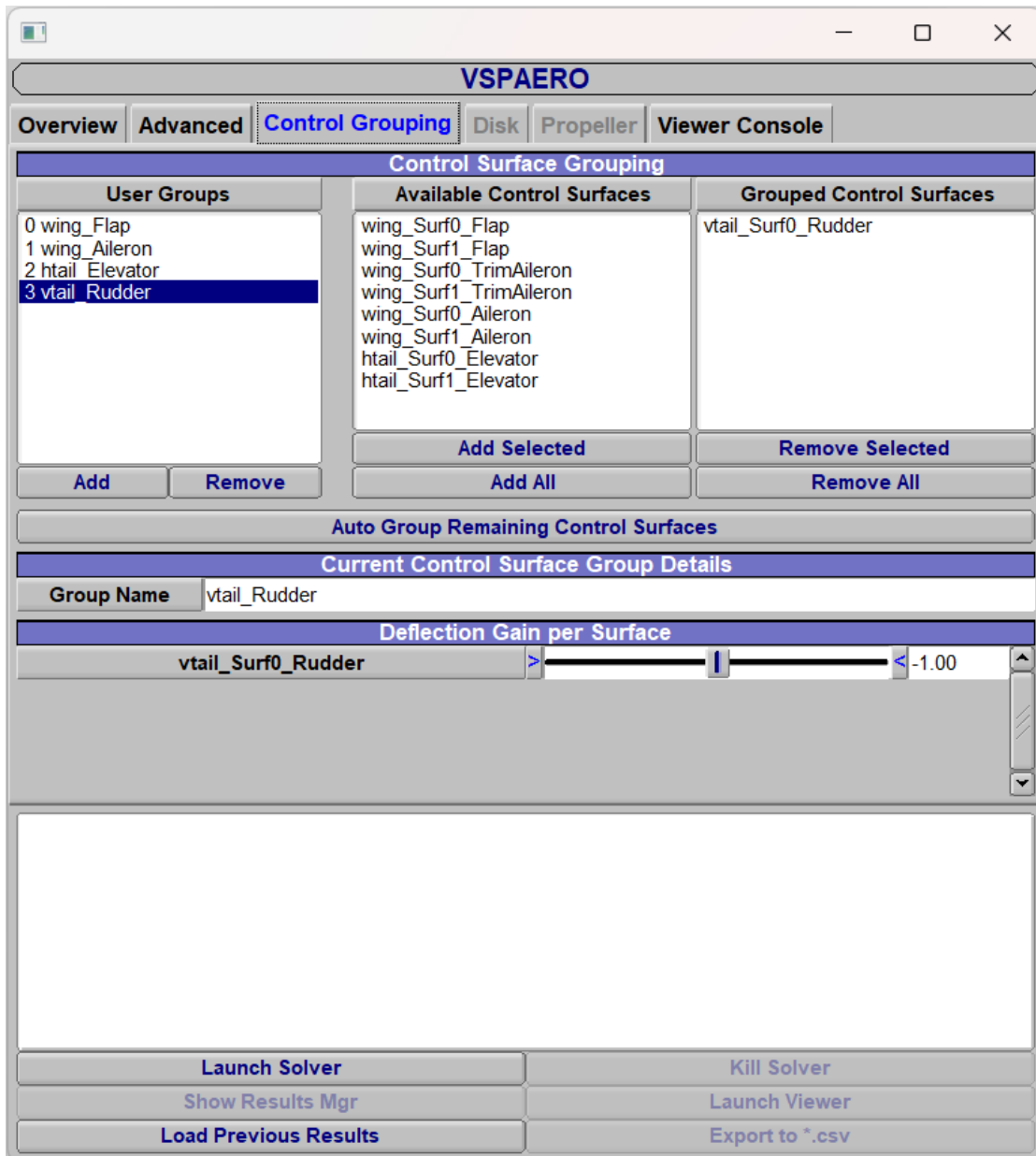


Figure 6.24 VSPAERO Control Grouping panel.

At this point one must be careful with the signs of the deflections because of the opposite conventions of the European system w.r.t. the American one (VSPAERO) in the elevator and rudder cases; the problem can be solved assuming the -1 the **Deflection Gain per Surface** for one of the elevators, such that a positive rotation corresponds to a downward deflection of both elevators.

Case	Delta	Units	CFx	CFy	CFz	CMx	CMy
#							
Base_Aero	0	n/a	0,000	-0,002	0,100	0,000	-0,051
Alpha	1	deg	-0,002	-0,002	0,191	0,000	-0,075
Beta	1	deg	0,000	-0,007	0,100	0,001	-0,051
Roll_Rate	1	rad/s	-0,014	0,001	0,100	0,076	-0,053
Pitch_Rate	1	rad/s	-0,006	-0,002	0,287	0,000	-0,352
Yaw_Rate	1	rad/s	-0,004	0,036	0,103	-0,006	-0,065
Mach	0,1	no_unit	0,000	-0,002	0,100	0,000	-0,051
wing_Flap	1	deg	0,001	-0,002	0,129	0,000	-0,050
wing_Aileron	1	deg	0,000	-0,002	0,100	0,005	-0,051
htail_Elevator	1	deg	0,001	-0,002	0,107	0,000	-0,071
vtail_Rudder	1	deg	0,000	0,000	0,100	0,000	-0,051
CMz	CL	CD	CS	CMI	CMm	CMn	
-0,001	0,100	0,000	-0,002	0,000	-0,051	0,001	
-0,001	0,191	0,002	-0,002	0,000	-0,075	0,001	
-0,002	0,100	0,000	-0,007	-0,001	-0,051	0,002	
0,001	0,100	-0,014	0,001	-0,076	-0,053	-0,001	
-0,001	0,287	-0,006	-0,002	0,000	-0,352	0,001	
0,013	0,103	-0,004	0,036	0,006	-0,065	-0,013	
-0,001	0,100	0,000	-0,002	0,000	-0,051	0,001	
-0,001	0,129	0,001	-0,002	0,000	-0,050	0,001	
-0,001	0,100	0,000	-0,002	-0,005	-0,051	0,001	
-0,001	0,107	0,001	-0,002	0,000	-0,071	0,001	
0,000	0,100	0,000	0,000	0,000	-0,051	0,000	

Table 6.5 Table of angle increments.

For the purpose of this study, it is important to highlight some derivatives:

- CL_α , $CM_{y\alpha}$, $CM_{x\beta}$, $CM_{z\beta}$ (stability derivatives).
- CM_{yq} , CM_{zr} , CM_{xp} (dynamic derivatives).
- CL_{δ_e} , $CM_{y\delta_e}$, $CM_{x\delta_r}$, $CM_{z\delta_r}$ (control derivatives).

Legend		
	stability derivatives	
	dynamic derivatives	
	control derivatives	

#	Base	Derivative:								
#	Aero	wrt	wrt	wrt	wrt	wrt	wrt	wrt	wrt	wrt
Coef	Total	Alpha	Beta	p	q	r	Mach	U	htail_Elevator	vtail_Rudder
#	-	per	per	per	per	per	per	per	per	per
#	-	rad	rad	rad	rad	rad	M	u	deg	deg
#										
CFx	0,00045	-0,12272	-0,00821	-0,09972	-0,37273	-0,02818	0,00003	0,00000	0,00053	0,00044
CFy	-0,00227	0,00094	-0,28606	0,02332	0,01045	0,26618	-0,00006	0,00000	-0,00227	0,00029
CFz	0,09992	5,22951	-0,00073	0,00354	10,68649	0,01828	0,00345	0,00000	0,10704	0,09993
CMx	0,00015	-0,00010	0,02986	0,52738	-0,00116	-0,04015	0,00000	0,00000	0,00015	-0,00003
CMy	-0,05085	-1,37051	-0,01636	-0,01495	-17,14623	-0,10036	-0,00094	0,00000	-0,07089	-0,05088
CMz	-0,00088	0,00038	-0,03760	0,01140	0,00414	0,09972	-0,00003	0,00000	-0,00088	0,00012
CL	0,09992	5,22954	-0,00073	0,00354	10,68649	0,01828	0,00345	0,00000	0,10704	0,09993
CD	0,00045	0,06847	-0,00095	-0,09972	-0,37273	-0,02818	0,00003	0,00000	0,00053	0,00044
CS	-0,00227	0,00094	-0,28569	0,02332	0,01045	0,26618	-0,00006	0,00000	-0,00227	0,00029
CMI	-0,00015	0,00010	-0,02986	-0,52738	0,00116	0,04015	0,00000	0,00000	-0,00015	0,00003
CMm	-0,05085	-1,37051	-0,01636	-0,01495	-17,14623	-0,10036	-0,00094	0,00000	-0,07089	-0,05088
CMn	0,00088	-0,00038	0,03760	-0,01140	-0,00414	-0,09972	0,00003	0,00000	0,00088	-0,00012

Table 6.6 Table of all derivatives.

The above values in Table 6.6 are all evaluated in a constructive reference system (x towards the stern, z upwards, y towards the right) with origin in the chosen pole (25% m.a.c.).

7. Conclusions

In the concluding part of this thesis, is to be subtilized that were made all the predetermined modeling and analysis and obtained approximate results on an aircraft that has proven to be a key player in global forest firefighting over the past 50 years. Despite the approximations related to the operational flow conditions and the geometry considered, the use of OpenVSP was preferred in order to have quickly and in a less refined way the different reliable results; the study carried out is therefore assimilable to a first approach to problems of this type, problems that in order to be treated in their entirety must be accompanied by experiments of another type that denote an adaptation to the reality of the facts, thus departing from what is a merely ideal study.

Bibliography

- [1] Ambrosino, De Martino, “Aerodynamic analysis and surrogate modelling of distributed propulsion on commuter and regional aircraft through VLM and CFD methods”, 2019.
- [2] Janes’s All the World’s Aircraft 2004-2005 Edited by Paul Jackson MRAeS
<https://shop.janes.com/>.
- [3] JPAD Modeller <https://www.smartup-engineering.com/jpad>.
- [4] OpenVSP site <https://openvsp.org/>.
- [5] VSPAERO Tutorial <https://openvsp.org/wiki/doku.php?id=vspaerotutorial>.
- [6] The OpenVSP discussion group <https://groups.google.com/g/openvsp>.
- [7] FLIGHT TEST: Bombardier 415 - The superscooper <https://www.flightglobal.com/flight-test-bombardier-415-the-superscooper/88562.article>.
- [8] Canadair CL-415 / Bombardier 415 - An ongoing RC-build
<http://starbase55.com/cl415/2020/11/05/status-update.html>.
- [9] Everything that You Need to Know about the Canadair CL-415 Infographic
<https://winair.ca/wp-content/uploads/2018/05/Everything-that-You-Need-to-Know-about-the-Canadair-CL-415-Infographic-Image.png>.
- [10] APP-C3-DESIGN_OF_SEAPLANES
https://booksite.elsevier.com/9780123973085/content/APP-C3-DESIGN_OF_SEAPLANES.pdf
- [11] Software testing: VSPAERO by Mariën, Floris <https://archive.org/details/TextMarien.pdf>